

Journal of Visualized Experiments

Probing Surface Electrochemical Activity of Nanomaterials using a Hybrid Atomic Force Microscope-Scanning Electrochemical Microscope (AFM-SECM)

--Manuscript Draft--

Article Type:	Invited Methods Article - JoVE Produced Video
Manuscript Number:	JoVE61111R2
Full Title:	Probing Surface Electrochemical Activity of Nanomaterials using a Hybrid Atomic Force Microscope-Scanning Electrochemical Microscope (AFM-SECM)
Section/Category:	JoVE Chemistry
Keywords:	Electrochemical activity, AFM-SECM, scanning electrochemical microscope, atomic force microscope, nanomaterial characterization
Corresponding Author:	Wen Zhang New Jersey Institute of Technology Newark, NJ UNITED STATES
Corresponding Author's Institution:	New Jersey Institute of Technology
Corresponding Author E-Mail:	wzhang81@njit.edu
Order of Authors:	Xiaonan Shi
	Qingquan Ma
	Taha Marhaba
	Wen Zhang
Additional Information:	
Question	Response
Please indicate whether this article will be Standard Access or Open Access.	Standard Access (US\$2,400)
Please indicate the city, state/province, and country where this article will be filmed. Please do not use abbreviations.	Newark, New Jersey, US, 07102

TITLE:

Probing Surface Electrochemical Activity of Nanomaterials using a Hybrid Atomic Force Microscope-Scanning Electrochemical Microscope (AFM-SECM)

AUTHORS:

Xiaonan Shi, Qingquan Ma, Taha Marhaba, Wen Zhang

Department of Civil and Environmental Engineering, New Jersey Institute of Technology, Newark, NJ

Email addresses of co-authors:

Xiaonan Shi (xs98@njit.edu)

Qingquan Ma (qm32@njit.edu)

Taha Marhaba (marhaba@njit.edu)

*Corresponding authors:

Wen Zhang (wen.zhang@njit.edu)

Keywords:

Electrochemical activity, AFM-SECM, scanning electrochemical microscope, atomic force microscope, nanomaterial characterization

Summary

Atomic force microscopy (AFM) combined with scanning electrochemical microscopy (SECM), namely, AFM-SECM, can be used to simultaneously acquire high-resolution topographical and electrochemical information on material surfaces at nanoscale. Such information is critical to understanding heterogeneous properties (e.g., reactivity, defects, and reaction sites) on local surfaces of nanomaterials, electrodes and biomaterials.

Abstract

Scanning electrochemical microscopy (SECM) is used to measure the local electrochemical behavior of liquid/solid, liquid/gas and liquid/liquid interfaces. Atomic force microscopy (AFM) is a versatile tool to characterize micro- and nanostructure in terms of topography and mechanical properties. However, conventional SECM or AFM provides limited laterally resolved information on electrical or electrochemical properties at nanoscale. For instance, the activity of a nanomaterial surface at crystal facet levels is difficult to resolve by conventional electrochemistry methods. This paper reports the application of a combination of AFM and SECM, namely, AFM-SECM, to probe nanoscale surface electrochemical activity while acquiring high-resolution topographical data. Such measurements are critical to understanding the relationship between nanostructure and reaction activity, which is relevant to a wide range of applications in material science, life science and chemical processes. The versatility of the combined AFM-SECM is demonstrated by mapping topographical and electrochemical properties of faceted nanoparticles (NPs) and nanobubbles (NBs), respectively. Compared to previously reported SECM imaging of

44 nanostructures, this AFM-SECM enables quantitative assessment of local surface activity or
45 reactivity with higher resolution of surface mapping.

46 **Introduction:**

47 Characterization of electrochemical (EC) behavior can provide critical insights into the kinetics
48 and mechanisms of interfacial reactions in diverse fields, such as biology^{1,2}, energy^{3,4}, material
49 synthesis⁵⁻⁷, and chemical process^{8,9}. Traditional EC measurements including electrochemical
50 impedance spectroscopy¹⁰, electrochemical noise methods¹¹, galvanostatic intermittent
51 titration¹², and cyclic voltammetry¹³ are usually performed at macroscopic scale and provide a
52 surface-average response. Thus, it is difficult to extract information on how electrochemical-
53 activity is distributed across a surface, but local scale surface properties in nanoscale are
54 especially important where nanomaterials are widely used. Therefore, new techniques capable
55 of simultaneously capturing both nanoscale multidimensional information and electrochemistry
56 are highly desirable.

57
58 Scanning electrochemical microscopy (SECM) is a widely used technique for measuring the
59 localized electrochemical activity of materials at micro- and nanoscales¹⁴. Typically, SECM uses an
60 ultra-microelectrode as a probe for detecting electroactive chemical species as it scans a sample
61 surface to spatially resolve local electrochemical properties¹⁵. The measured current at the probe
62 is produced by reduction (or oxidation) of the mediator species, and this current is an indicator
63 of the electrochemical reactivity at the surface of the sample. SECM has evolved significantly after
64 its first inception in 1989^{16,17} but it is still challenged by two main limitations. Since EC signals are
65 typically sensitive to tip-substrate interaction characteristics, one limitation of SECM is that
66 keeping the probe at a constant height prevents a direct correlation of electrochemical activity
67 with the surface landscape, due to the convolution of topography with the collected EC
68 information¹⁸. Second, it is difficult for a commercial SECM system to obtain sub-micrometer (μm)
69 image resolution as the spatial resolution is partially determined by the probe dimensions, which
70 is on the micrometer scale¹⁹. Therefore, nanoelectrodes, the electrodes with a diameter in the
71 nanometer range, are increasingly used in SECM to achieve a resolution below the sub-
72 micrometer scale²⁰⁻²³.

73
74 To provide a constant tip-substrate distance control and obtain a higher spatial electrochemical
75 resolution, several hybrid techniques of SECM have been used, such as ion conductance
76 positioning²⁴, shear force positioning²⁵, alternating current SECM²⁶, and atomic force microscopy
77 (AFM) positioning. Among these instrumentations, SECM integrating AFM positioning (AFM-
78 SECM) has become a highly promising approach. As AFM can provide fixed tip-substrate distances,
79 the integrated AFM-SECM technique enables simultaneous acquisition of nanoscale surface
80 structural and electrochemical information through mapping or sample sweeping with the sharp
81 AFM tips. Since the first successful operation of AFM-SECM by MacPherson and Unwin in 1996²⁷,
82 significant improvements have been achieved on probe design and fabrication, as well as its
83 applications in various research fields such as electrochemistry in chemical and biological
84 processes. For example, AFM-SECM has been implemented for imaging composite material
85 surfaces, such as noble metal nanoparticles²⁸, functionalized or dimensionally stable
86

electrodes^{29,30}, and electronic devices³¹. AFM-SECM can map the electrochemically active sites from the tip current image.

Simultaneous topographical and electrochemical measurements could also be achieved by other techniques such as conductive AFM³²⁻³⁵, electrochemical AFM (EC-AFM)³⁶⁻³⁹, scanning ion conductance microscopy-scanning electrochemical microscopy (SICM-SECM)^{24,40}, and scanning electrochemical cell microscopy (SECCM)^{41,42}. The comparison between these techniques has been discussed in a review paper¹. The aim of the present work was to employ SECM-AFM to demonstrate the electrochemical mapping and measurement on faceted crystalline cuprous oxide nanomaterials and nanobubbles in water. Faceted nanomaterials are widely synthesized for metal oxide catalysts in clean energy applications because the facets with distinctive crystallographic features have distinctive surface atomic structures and further dominate their catalytic properties. Moreover, we also measured and compared the electrochemical behavior at the liquid/gas interfaces for surface nanobubbles (NBs) on gold substrates. NBs are bubbles with a diameter of <1 μm (also known as ultrafine bubbles)⁴³, and they elicit many intriguing properties^{44,45}, including long residence times in the solutions^{46,47} and higher efficiency of gas mass transfer^{46,48}. Furthermore, the collapse of NBs creates shock waves and the formation of hydroxyl radicals ($\bullet\text{OH}$)⁴⁹⁻⁵². We measured the electrochemical reactivity of oxygen NBs in the solution to better understand the fundamental chemical properties of NBs.

PROTOCOL:

1. Sample preparation

1.1. Preparation of faceted Cu_2O nanoparticles and deposition on silicon substrate

1.1.1. Dissolve 0.175 g of $\text{CuCl}_2 \cdot 2\text{H}_2\text{O}$ (99.9%) into 100 mL of deionized (DI) water to generate an aqueous solution of 10 mM CuCl_2 .

1.1.2. Add 10.0 mL of 2.0 M NaOH and 10 mL of 0.6 M ascorbic acid dropwise into the CuCl_2 solution.

1.1.3. Heat the solution in a 250 mL round-bottom flask under constant stirring in a 55 $^\circ\text{C}$ water bath for 3 h.

1.1.4. Collect the resulting precipitate by centrifugation (5,000 $\times g$ for 15 min), followed by washing with DI water 3 times and ethanol twice to remove the residual inorganic ions and polymers.

1.1.4. Dry precipitate in vacuum at 60 $^\circ\text{C}$ for 5 h⁵³.

1.1.5. Use the prepared silicon wafer as the substrate to deposit Cu_2O nanoparticles as illustrated in **Figure 1A** using epoxy to ensure the testing.

Caution: The silicon wafer ($\varnothing 3''$ Silicon wafer, Type P/<111>) was cut into a single piece of 38 mm x 38 mm, followed by washing using ethanol, methanol and DI water to remove organic and inorganic contaminants.

1.1.6. Directly deposit 10 μL of epoxy on the cleaned silicon wafer using a pipette tip and tile with a clean glass slide. After about 5 min, drop 10 μL of the nanoparticles/water suspension (10 mg L^{-1}) on different epoxy-coated silicon wafer substrates, separately. The four different red spots shown in **Figure 1B** indicate the potential position of the deposited nanoparticles.

1.1.7. Vacuum dry the substrate at 40 $^{\circ}\text{C}$ for 6 h.

1.1.8. Place the sample substrate into the EC sample cell (**Figure 4**) to be filled with 1.8 mL of a 0.1 M KCl containing 10 mM $\text{Ru}(\text{NH}_3)_6\text{Cl}_3$ (98%).

1.2. Preparation of NBs

1.2.1. Generate oxygen nanobubbles by direct injection of compressed oxygen (purity 99.999%) through a tubular ceramic membrane (100 nm pore size, WFA0.1) into DI water.

NOTE: The gas was injected continuously under a pressure of 414 kPa and a flow of 0.45 $\text{L}\cdot\text{m}^{-1}$ until reaching stable bubble size distribution as reported elsewhere⁵⁴.

1.2.2. Add 1.8 mL of the water suspension of NBs on a gold substrate in the EC sample cell and stabilize for 10 min.

NOTE: Fresh 40 mm x 40 mm gold plates (Au on Si) were used as the substrate to immobilize NBs.

1.2.3. Decant 0.9 mL of NB suspension and replace with 0.9 mL of a 10 mM $\text{Ru}(\text{NH}_3)_6\text{Cl}_3$ solution in 0.1 M KCl.

2. Setup of AFM-SECM

NOTE: AFM was used in the presented AFM-SECM measurements. To perform the EC analyses, the AFM was equipped with a bipotentiostat and SECM accessories. As shown in **Figure S1**, the bipotentiostat was connected to the AFM controller and both the potentiostat and AFM were connected to the same computer. The accessories include an SECM chuck, an SECM probe holder with protective boot, and a strain-release module with a resistance selector (10 $\text{M}\Omega$ resistance was used) to limit the maximum current flow⁵⁵. As shown in **Figure 2**, the AFM-SECM probes have a tip radius of 25 nm and a tip height of 215 nm. The sample acted as a working electrode, which shares the same pseudo-reference using the Ag wire electrode (25 mm diameter) and the counter electrode of a Pt wire (25 mm in diameter). The probe and the sample could be biased at different potentials (vs the Ag wire pseudo-reference electrode) to enable different redox reactions. In the presented work, the tip reduces the $[\text{Ru}(\text{NH}_3)_6]^{3+}$ to $[\text{Ru}(\text{NH}_3)_6]^{2+}$ at -400 mV versus an Ag wire pseudo-reference electrode.

2.1. Replace the existing sample chuck with SECM chuck and screw the chuck in place using two M3 x 6 mm socket head cap screws and a 2.5 mm hex wrench (**Figure 3A**).

2.2. Connect the temperature control cable to the SECM chuck, and connect the low-noise SECM cables to the spring connector block (color to color) and switch block (**Figure 3B**).

NOTE: The switch needs to be kept on the right side during SECM testing.

2.3. Install the strain-release module onto the AFM scanner and also connect it to the working electrode connector on the spring connector block with extension cable (**Figure 3C**).

2.4. Assemble the EC sample cell.

2.4.1. Put the insert onto the top ring (**Figure 4A**).

2.4.2. Assemble two O-rings onto the bottom groove and top groove of the insert, respectively (**Figure 4B** and **Figure 4C**).

2.4.3. Put a glass cover onto the top ring top and then tighten by four screws lightly and diagonally (**Figure 4D**).

2.4.4. Use a hard sharp wire with a 24 mm diameter (**Figure 4E**) to poke two holes in the O-ring through two channels of plastic part on top ring (**Figure 4F**).

2.4.5. Insert Ag wire and Pt wire through the hole on the O-ring, and curve the Pt wire to a circle in EC sample cell as shown in **Figure 4G**.

2.4.6. To seal the EC sample cell top part, press the assembled EC sample cell down on the EC sample cell bottom to make the O-ring fully contact the glass cover (**Figure 4H**).

2.4.7. Place the top part of the EC sample cell upside-down and face the test sample (or substrate) downward so that the spring-loaded pins (pogo pins) touch the sample surface as shown in **Figure 4I** and **Figure 4J**. The test sample should be covering the O-ring to make EC sample cell bottom part seal.

2.4.8. Put the EC sample cell bottom on and tighten diagonally with right length screw (**Figure 4K**).

3. Operation of AFM-SECM

3.1. Initialization of the AFM and bipotentiostat instruments

3.1.1 Double click the two software icons to initialize the AFM system and the bipotentiostat control interface.

3.2. Loading SECM Probe

3.2.1 Prepare the ESD field service package including antistatic pad, electrostatic discharge (ESD) protective probe stand, wearable anti-static gloves and wrist strap (**Figure 5A**). **Figure 5B** shows the connection of the ESD monitor with wrist strap.

NOTE: The ESD monitor beeps when the red pad is connected with ground. The beep will stop when user wears the wrist strap.

3.2.2 To prevent AFM scanner from exposure to liquid, use a protective boot (**Figure 6A**) during AFM-SECM testing. Put the probe holder onto the ESD protective probe stand (**Figure 6B**). Use a pair of plastic tweezers to attach the protective boot to the tip holder (**Figure 6C**). Then, align the small cut in the protective boot to the notch in the probe holder as illustrated in **Figure 6D**.

3.2.3 Open the box of AFM-SECM probes (**Figure 7A**) using a tip tweezer (green color) to grab the probe from both sides of the grooves (**Figure 7B**). While using the disk gripper (silver color) to hold the probe holder on the stand, put the probe wire into the hole of the stand, and then slide the probe into the slot of the probe holder (**Figure 7C**). After the probe is inside the slot, use the flat end of the tweezer to push it in. Make sure the probe is completely in the tip holder (**Figure 7D**).

3.2.4. As shown in **Figure 8A**, attach the whole probe holder (including the holder-boot) to the scanner.

3.2.5. Use the Teflon tip tweezer to grab the wire right below the copper ring and connect it to the module (**Figure 8B**).

3.2.6. Put the scanner back to the dovetail.

3.3. Loading the sample cell

3.3.1. After assembling the test sample (or substrate) in the EC sample cell, which was mentioned in Section 2.4, put the EC sample cell on the central point of the SECM chuck and the pseudo-reference electrode (Ag wire) and connect the counterelectrode (Pt wire) to the spring connector block (**Figure 3**). The EC sample cell is magnetically attached to the chuck.

3.4. SECM software preparation before imaging

3.4.1. In the AFM-SECM software, select SECM- PeakForce QNM to load the workspace (**Figure S2**).

3.4.2. In **Setup**, load the SECM probe, and then align a laser on the tip using an alignment station.

3.4.3. Go to **Navigation (Figure S3)**. Move the scanner downwards slowly to focus on the sample surface. Adjust the position of EC sample cell slightly to make sure the scanner would not touch the glass cover of EC sample cell while moving. After focusing on the sample, click **Update Blind Engage Position**.

Caution: Different samples have different heights, so it is necessary to update the blind engage position after changing a sample.

3.4.4. Click **Move to Add Fluid Position**.

3.4.5. Add ~1.8 mL of the buffer solution into the EC sample cell, to make sure the level of the solution is lower than the glass cover. If the water level is over the glass cover, water can creep to the scanner and cause an electric short and break the scanner. Wait for another 5 minutes and use a pipette to agitate the solution to remove bubbles.

NOTE: The buffer solution (10 mM $[\text{Ru}(\text{NH}_3)_6]^{3+}$ with supporting electrolyte of 0.1 M KCl) should be constantly stored in a refrigerator after preparation. Use a syringe with filter (no larger than 1 μm pore size) to filter the solution before using it.

3.4.6. Click **Move to Blind Engage Position**. The tip will move back into the buffer solution. Adjust the laser slightly to make sure the laser is aligned on the tip.

3.4.7. Open CHI software. As shown in **Figure S4**, click on the **Technique** command on the toolbar to open up the tech selector and select **Open Circuit Potential – Time**. Use the default setting (Run time as 400 s) for OCP measurement and run the OCP measurement.

NOTE: The potential showed in OCP test should be near zero stably.

3.4.8. Click the **Technique** command again and run **Cyclic Voltammetry (CV)**, as shown in **Figure S5 and Figure S6**.

NOTE: Set up the parameters as below. Set “sweep segments” to a larger number if needed. The “init E/Final E” should be as the same as the potential value from OCP measurement and “High E” and “Low E” could be +0.3 V or –0.3 V of “init E/Final E”, respectively. Here we use 0 V as initial and high E and -0.4 V as Low and Final E. The scan rate was 0.05 V/s and the sensitivity was 1 e-009. Run the CV test, the highest current (i) measured here should be 0.3-1.2 nA for 10 mM $[\text{Ru}(\text{NH}_3)_6]^{3+}$.

3.5. SECM Imaging

3.5.1. Go back to the AFM-SECM software. Since the tip is already in the liquid, click **Engage**.

3.5.2. After scanning, turn on lift mode (Lift by Sensor) with a lift height of 100 nm and adjust the lift height based on the sample roughness.

3.5.3. In CHI software, run a chronoamperometry with parameters shown in **Figure S7**. Set the initial E as -0.4 V, the pulse width as 1000 seconds (which is the maximum number accepted by the system), and the sensitivity the same with CV scan.

NOTE: The chronoamperometry technique was chosen because of the absence of amperometric i-t technique in the presented bi-potentiostat.

3.5.4. With the CHI program running, go back to AFM-SECM software, check the real-time reading on the strip chart and click on **Start (Figure S8)**. The reading will be updated in real-time. Then both topography imaging and current imaging process will begin. Save images in the AFM-SECM software.

3.6. Check approach curve

3.6.1. Engage the tip on sample or substrate region with a scan size of 1 μm .

3.6.2. Run the **Chronoamperometry** as mentioned in 3.5.3.

3.6.3. Go back to AFM-SECM Software and select the command **Go To Ramp**.

3.6.4. Click **Ramp**. An approach curve would be recorded in the AFM-SECM software.

3.7. Tip cleaning

3.7.1. Using the EC sample cell as a clean water container. Move the tip in and out of the liquid using blind engage functions in the navigation panel. Change the clean water three times. After this three-time cleaning, using clean wipes to carefully remove residual water from the probe holder and put the probe back in the probe box.

Caution: After imaging, the AFM-SECM probe needs to be carefully cleaned. Never use water coming out from the wash bottle to clean the probe as the electrostatic charge might damage the probe.

REPRESENTATIVE RESULTS

Topography and current imaging of ONBs by AFM-SECM

Previous studies that characterized NBs with AFM only reported topography images to reveal the size and distribution of NBs immobilized on a solid substrate^{56,57}. The experiments here revealed both morphological and electrochemical information. Individual oxygen nanobubbles (ONBs) can be clearly identified in **Figure 9**, which provides the topography as well as the tip current mapping or information. The tip current was generated by the redox reaction of $[\text{Ru}(\text{NH}_3)_6]^{3+}$ that is reduced to $[\text{Ru}(\text{NH}_3)_6]^{2+}$ at the tip under a bias potential at -0.4 V, as depicted in **Figure 9C**. A comparison of the topography and current image shows the good correlation between the locations of the NBs and the current spots. This result confirms that ONBs could facilitate the

diffusion and mass transfer of $[\text{Ru}(\text{NH}_3)_6]^{3+}$ from the bulk solution to the tip area⁵⁸ and result in a higher current (relative to the substrate background current of 6 pA) when the AFM-SECM tip scanned over NBs⁵⁹.

Topography and current imaging of Cu_2O NPs by AFM-SECM

The topography and current images of Cu_2O nanoparticles are presented in **Figure 10**. The tip current was generated due to the redox reaction of $[\text{Ru}(\text{NH}_3)_6]^{3+}$, which are also reduced at the tip with a potential at -0.4 V, as depicted in **Figure 10C**. The nanoparticle is about 500-1000 nm in size. The presented topography image was processed with a 1st order flattening treatment. The particle size determined by AFM is comparable to that obtained from the SEM image. The length or width is slightly larger than the height of the nanoparticles (around 500 nm) due to the tip convolution effect, a well-known artifact in the AFM imaging process that causes the overestimation of the object dimension by a finite-sized AFM tip⁶⁰. In this study, as the Cu_2O nanoparticle has a sharp octahedron shape, the AFM tip may fail to touch the steep sidewall and bottom, and this convolution effect can account for many lateral broadening of the surface⁶¹. **Figure 10B** indicates that the nanoparticle visible in the topography image is associated with evident electric current “spot” in current image, whereas the background current (~10 pA) corresponds to the flat silicon substrate.

CV and Approach curves of Cu_2O NPs

Figure 11A shows five representative CV curves of the AFM-SECM tip with the tip at around 1 mm away from the substrate in 10 mM $[\text{Ru}(\text{NH}_3)_6]^{3+}$ and 0.1 M KCl. The diffusion-limited tip current (~1.2 nA) did not decrease with time. **Figure 11A** shows the CV curve at a scan rate as 50 mV s⁻¹, which confirms the bias potential of -0.4 V vs Ag/AgCl led to the maximum plateau tip current due to the reduction reaction of $[\text{Ru}(\text{NH}_3)_6]^{3+}$.

Figure 11B shows the changes of the tip current as the tip move towards the sample surface. The AFM-SECM tip approached the substrate surface in the Z direction until it reached a setpoint (5 nN in this work) that indicates the physical tip-substrate contact or bending as a result of the contact^{62,63}. The current on the plots were normalized to i_0 ($i_0=3.385$ nA), which is defined as the tip current measured when the tip is 1 μm above the sample surface. The tip was biased at -0.4 V vs Ag/AgCl in electrolyte containing 10 mM $[\text{Ru}(\text{NH}_3)_6]^{3+}$ and 0.1 M KCl. The normalized tip current increased with the decreasing tip-sample distance. At <8 nm, the tip was in contact with the nanoparticle surface and the normalized tip current increased sharply, probably because the negatively charged Si surface would result in an increased local concentration of $[\text{Ru}(\text{NH}_3)_6]^{3+}$ near the surface.

Figure and Table legends

Figure 1. Deposition of Cu_2O nanoparticles on a silicon wafer.

Figure 2. Schematic of AFM-SECM system

Figure 3. Installation procedure for SECM chuck and other accessories.

Figure 4. Assemblage procedure of the EC sample cell.

Figure 5. The ESD field service package. (A) Parts of ESD protective parts; **(B)** Connections of ESD monitor, wrist strap and ground wire.

Figure 6. Attachment procedure for the protective boot onto the probe holder

Figure 7. Loading the SECM probe to the probe holder

Figure 8. The SECM Probe. (A) Attach the probe-holder-boot assembly to the scanner; **(B)** Connection of probe to the strain released module.

Figure 9. Simultaneously acquired topography (A) and tip current (B) images of oxygen NBs in electrolyte containing 10 mM [Ru(NH₃)₆]³⁺ and 0.1 M KCl. The tip (end tip radius is 25nm) was biased at -0.4V. **(C)** Schematic illustration of AFM-SECM measurement of NBs

Figure 10. Simultaneously acquired topography (A) and tip current (B) images of Cu₂O nanoparticles in electrolyte containing 10 mM [Ru(NH₃)₆]³⁺ and 0.1 M KCl. The tip (end tip radius is 25nm) was biased at -0.4V **(C)** Schematic illustration of AFM-SECM measurement of NPs.

Figure 11. CV and Approach curves of Cu₂O NPs. (A) Five CV scan in 10 mM [Ru(NH₃)₆]³⁺ and 0.1 M KCl. **(B)** Approach curves of nanoelectrode probe on Cu₂O nanoparticle surface.

Table 1. Examples of redox mediators used in literature.

Figure S1. Photo showing connection between the bipotentiostat and the AFM controller.

Figure S2. Load the PeakForce SECM workspace in the software

Figure S3. Navigation panel for SECM workspace.

Figure S4. Run Open Circuit Potential – Time

Figure S5. Run Cyclic Voltammetry

Figure S6. Parameter setting for cyclic voltammetry measurement

Figure S7. Parameters for a Chronoamperometry measurement

Figure S8. Start current reading in AFM-SECM software

Figure S9. Parameters for Amperometric i-t technique

Discussion

A combined AFM-SECM technique that enables high-resolution multimodal imaging has been described in this protocol. This technique allows for topography to be mapped simultaneously with the SECM current collected or mapped on single nanoparticles or nanobubbles. Experiments were performed using commercial probes. These probes were designed to provide chemical compatibility with a wide range of electrochemical environments, electrochemical performance, mechanical stability, and multiple-cycle handling¹⁸. However, the stability and durability of the AFM-SECM are critical for the measurement of the electrochemical information with reliable and high resolution. As a result, the steps mentioned in steps 3.2 and 3.7 are critical to protecting the AFM-SECM tip from destroying by electrostatic discharge. Detailed discussion related to specific protocol steps are described as well.

In step 3.4.5, 10 mM $[\text{Ru}(\text{NH}_3)_6]^{3+}$ with supporting electrolyte of 0.1 M KCl was used in the presented test. 5-10 mM is a commonly used concentration of $[\text{Ru}(\text{NH}_3)_6]^{3+}$ in literature to obtain good current signals³⁰. More examples of commonly used redox mediators in AFM-SECM measurements are summarized in the discussion (**Table 1**).

In step 3.4.6, the quality and stability of electrodes are confirmed with the OCP measurement. If the potential measured in OCP is not near zero or unstable, then the counter and pseudo-reference electrodes must be checked. The possible reasons for unstable OCP may be the attachment of bubbles on the electrodes or the electrodes not immersed in liquid.

In step 3.4.8, the potential range mentioned here “High E” and “Low E” could be +0.3 V or -0.3 V of “init E/Final E” is a safe choice to start the CV test. Then, the potential range could be adjusted based on the potential value that led to a plateau current in the CV curve. Scan rate could vary between 0.01 V/s to 0.1 V/s. A higher scan rate attributes to a higher sensibility, but the charging current would also increase. Also, at high scan rates the voltammograms presented distorted shapes⁶⁴. A higher sensitivity value should be selected as long as CV test does not show “overflow”. If an “overflow” message showed, then the sensitivity should be decreased.

In step 3.5.2, for imaging, the AFM-SECM imaging process was performed using a lift scan mode with a lift height typically 40-150 nm. If a lower lift height was selected, then there may be a possibility for tip crashing onto the sample surface. If the lift height was too high, then it may decrease the current imaging resolution since the tip is far away from the sample surface.

In step 3.5.3 in the presented measurement protocol, -0.4 V versus Ag/AgCl (-0.18V versus NHE) was chosen to perform the reduction of $[\text{Ru}(\text{NH}_3)_6]^{3+}$. The probe may reduce the $[\text{Ru}(\text{NH}_3)_6]^{3+}$ to $[\text{Ru}(\text{NH}_3)_6]^{2+}$ at -0.35 to -0.5 V vs Ag wire pseudo-reference electrode, while the sample maybe biased at 0 to -0.1 V for $[\text{Ru}(\text{NH}_3)_6]^{3+}$ regeneration. This value depends on the plateau current measured in the CV scan. It will also vary with different redox mediators as summarized in **Table 1**.

Also, the chronoamperometry technique was chosen because of the absence of Amperometric i-t technique in the presented bi-potentiostat. If readers have a bi-potentiostat that supports

Amperometric i-t technique, they can set the i-t technique as shown in **Figure S9**. The run time was selected as 2000 seconds to make sure it is enough for at least one current imaging process in AFM-SECM.

Moreover, sample preparation is very important as well since the solid particles must be immobilized on the substrate completely so that particles do not detach during the imaging process. Moreover, to scan or probe electrochemical or electrical properties of sample surfaces (e.g., electrode), the binding between samples and substrates needs to ensure the electrical conductivity. The sample preparation methods should be useful and referable to a wide range of applications, especially for nano-objects characterization; however, sample immobilization methods may vary with specific samples^{65,66}. Overall, we demonstrated that AFM-SECM enables high-resolution imaging of oxygen NBs and Cu₂O nanoparticles. Clearly, this AFM-SECM protocol is anticipated to play important roles in interfacial electrochemical analysis and will have broad applications in different research fields, such as material science, chemistry, and life science^{1,19}.

Acknowledgment

This work is funded by the national science foundation (Award Number: 1756444) via Biological & Environmental Interfaces of Nano Materials, the USDA National Institute of Food and Agriculture, AFRI project [2018-07549] and Assistance Agreement No. 83945101-0 awarded by the U.S. Environmental Protection Agency to New Jersey Institute of Technology. It has not been formally reviewed by EPA. The views expressed in this document are solely those of authors and do not necessarily reflect those of the Agency. EPA does not endorse any products or commercial services mentioned in this publication. The authors also thank Undergraduate Research and Innovation program (URI) Phase-1 & Phase-2 at New Jersey Institute of Technology.

Disclosures

The authors have nothing to disclose.

References

- 1 Shi, X., Qing, W., Marhaba, T., Zhang, W. Atomic Force Microscopy-Scanning Electrochemical Microscopy (AFM-SECM) for Nanoscale Topographical and Electrochemical Characterization: Principles, Applications and Perspectives. *Electrochimica Acta*. 135472 (2019).
- 2 Aazam, E. S., Ghoneim, M. M., El-Attar, M. A. Synthesis, characterization, electrochemical behavior, and biological activity of bisazomethine dye derived from 2, 3-diaminomaleonitrile and 2-hydroxy-1-naphthaldehyde and its zinc complex. *Journal of Coordination Chemistry*. **64** (14), 2506-2520 (2011).
- 3 Shukla, A., Sampath, S., Vijayamohanan, K. Electrochemical supercapacitors: Energy storage beyond batteries. *Current science*. **79** (12), 1656-1661 (2000).
- 4 Kötz, R., Carlen, M. Principles and applications of electrochemical capacitors. *Electrochimica Acta*. **45** (15-16), 2483-2498 (2000).
- 5 Botte, G. G. Electrochemical manufacturing in the chemical industry. *The Electrochemical Society Interface*. **23** (3), 49-55 (2014).
- 6 Kongsricharoern, N., Polprasert, C. Electrochemical precipitation of chromium (Cr6+) from an electroplating wastewater. *Water Science and Technology*. **31** (9), 109-117 (1995).

- 7 Datta, M., Landolt, D. Fundamental aspects and applications of electrochemical microfabrication. *Electrochimica Acta*. **45** (15-16), 2535-2558 (2000).
- 8 Wang, S., George, K., Nesic, S. High pressure CO₂ corrosion electrochemistry and the effect of acetic acid. *Corrosion/2004, paper*. **4375** (2004).
- 9 Song, G.-L. in *Corrosion of Magnesium alloys*. 3-65 (Elsevier, 2011).
- 10 Bellezze, T., Giuliani, G., Viceré, A., Roventi, G. Study of stainless steels corrosion in a strong acid mixture. Part 2: anodic selective dissolution, weight loss and electrochemical impedance spectroscopy tests. *Corrosion Science*. **130** 12-21 (2018).
- 11 Ehsani, A. et al. Evaluation of Thymus vulgaris plant extract as an eco-friendly corrosion inhibitor for stainless steel 304 in acidic solution by means of electrochemical impedance spectroscopy, electrochemical noise analysis and density functional theory. *Journal of Colloid and Interface Science*. **490** 444-451 (2017).
- 12 Cui, Z. H., Guo, X. X., Li, H. Equilibrium voltage and overpotential variation of nonaqueous Li-O₂ batteries using the galvanostatic intermittent titration technique. *Energy & Environmental Science*. **8** (1), 182-187 (2015).
- 13 Elgrishi, N. et al. A Practical Beginner's Guide to Cyclic Voltammetry. *Journal of Chemical Education*. **95** (2), 197-206 (2018).
- 14 Amemiya, S., Bard, A. J., Fan, F.-R. F., Mirkin, M. V., Unwin, P. R. Scanning Electrochemical Microscopy. *Annual Review of Analytical Chemistry*. **1** (1), 95-131 (2008).
- 15 Mirkin, M. V., Nogala, W., Velmurugan, J., Wang, Y. Scanning electrochemical microscopy in the 21st century. Update 1: five years after. *Physical Chemistry Chemical Physics*. **13** (48), 21196-21212 (2011).
- 16 Bard, A. J., Fan, F. R. F., Kwak, J., Lev, O. Scanning electrochemical microscopy. Introduction and principles. *Analytical Chemistry*. **61** (2), 132-138 (1989).
- 17 Engstrom, R. C., Pharr, C. M. Scanning electrochemical microscopy. *Analytical Chemistry*. **61** (19), 1099A-1104A (1989).
- 18 Nellist, M. R. et al. Atomic force microscopy with nanoelectrode tips for high resolution electrochemical, nanoadhesion and nanoelectrical imaging. *Nanotechnology*. **28** (9), 095711 (2017).
- 19 Patel, A. N., Kranz, C. (Multi) functional atomic force microscopy imaging. *Annual Review of Analytical Chemistry*. **11** 329-350 (2018).
- 20 Ufheil, J., Heß, C., Borgwarth, K., Heinze, J. Nanostructuring and nanoanalysis by scanning electrochemical microscopy (SECM). *Physical Chemistry Chemical Physics*. **7** (17), 3185-3190 (2005).
- 21 Bergner, S., Wegener, J., Matysik, F.-M. Simultaneous imaging and chemical attack of a single living cell within a confluent cell monolayer by means of scanning electrochemical microscopy. *Analytical Chemistry*. **83** (1), 169-174 (2011).
- 22 Hu, K. et al. Platinized carbon nanoelectrodes as potentiometric and amperometric SECM probes. *Journal of Solid State Electrochemistry*. **17** (12), 2971-2977 (2013).
- 23 Kranz, C. Recent advancements in nanoelectrodes and nanopipettes used in combined scanning electrochemical microscopy techniques. *Analyst*. **139** (2), 336-352 (2014).
- 24 Morris, C. A., Chen, C.-C., Baker, L. A. Transport of redox probes through single pores measured by scanning electrochemical-scanning ion conductance microscopy (SECM-SICM). *Analyst*. **137** (13), 2933-2938 (2012).

- 25 Ludwig, M., Kranz, C., Schuhmann, W., Gaub, H. E. Topography feedback mechanism for the scanning electrochemical microscope based on hydrodynamic forces between tip and sample. *Review of Scientific Instruments*. **66** (4), 2857-2860 (1995).
- 26 Eckhard, K., Schuhmann, W. Alternating current techniques in scanning electrochemical microscopy (AC-SECM). *Analyst*. **133** (11), 1486-1497 (2008).
- 27 Macpherson, J. V., Unwin, P. R., Hillier, A. C., Bard, A. J. In-situ imaging of ionic crystal dissolution using an integrated electrochemical/AFM probe. *Journal of the American Chemical Society*. **118** (27), 6445-6452 (1996).
- 28 Huang, K., Anne, A., Bahri, M. A., Demaille, C. Probing Individual Redox PEGylated Gold Nanoparticles by Electrochemical–Atomic Force Microscopy. *ACS Nano*. **7** (5), 4151-4163 (2013).
- 29 Chennit, K. et al. Electrochemical Imaging of Dense Molecular Nanoarrays. *Analytical Chemistry*. **89** (20), 11061-11069 (2017).
- 30 Jiang, J. et al. Nanoelectrical and Nanoelectrochemical Imaging of Pt/p-Si and Pt/p+-Si Electrodes. *ChemSusChem*. **10** (22), 4657-4663 (2017).
- 31 Knittel, P., Mizaikoff, B., Kranz, C. Simultaneous nanomechanical and electrochemical mapping: combining peak force tapping atomic force microscopy with scanning electrochemical microscopy. *Analytical Chemistry*. **88** (12), 6174-6178 (2016).
- 32 Quist, A. P. et al. Atomic force microscopy imaging and electrical recording of lipid bilayers supported over microfabricated silicon chip nanopores: Lab-on-a-chip system for lipid membranes and ion channels. *Langmuir*. **23** (3), 1375-1380 (2007).
- 33 Cohen, H. et al. Electrical characterization of self-assembled single- and double-stranded DNA monolayers using conductive AFM. *Faraday Discussions*. **131** (0), 367-376 (2006).
- 34 Chung, J. W. et al. Single-crystalline organic nanowires with large mobility and strong fluorescence emission: a conductive-AFM and space-charge-limited-current study. *Journal of Materials Chemistry*. **19** (33), 5920-5925 (2009).
- 35 Guo, D.-Z., Hou, S.-M., Zhang, G.-M., Xue, Z.-Q. Conductance fluctuation and degeneracy in nanocontact between a conductive AFM tip and a granular surface under small-load conditions. *Applied Surface Science*. **252** (14), 5149-5157 (2006).
- 36 Rocca, E., Bertrand, G., Rapin, C., Labrune, J. C. Inhibition of copper aqueous corrosion by non-toxic linear sodium heptanoate: mechanism and ECAFM study. *Journal of Electroanalytical Chemistry*. **503** (1), 133-140 (2001).
- 37 Toma, F. M. et al. Mechanistic insights into chemical and photochemical transformations of bismuth vanadate photoanodes. *Nature Communications*. **7** 12012-12012 (2016).
- 38 Kouzeki, T., Tatzono, S., Yanagi, H. Electrochromism of Orientation-Controlled Naphthalocyanine Thin Films. *The Journal of Physical Chemistry*. **100** (51), 20097-20102 (1996).
- 39 Yamaguchi, Y., Shiota, M., Nakayama, Y., Hirai, N., Hara, S. Combined in situ EC-AFM and CV measurement study on lead electrode for lead–acid batteries. *Journal of Power Sources*. **93** (1), 104-111 (2001).
- 40 Comstock, D. J., Elam, J. W., Pellin, M. J., Hersam, M. C. Integrated Ultramicroelectrode–Nanopipet Probe for Concurrent Scanning Electrochemical Microscopy and Scanning Ion Conductance Microscopy. *Analytical Chemistry*. **82** (4), 1270-1276 (2010).
- 41 Ebejer, N., Schnipper, M., Colburn, A. W., Edwards, M. A., Unwin, P. R. Localized High Resolution Electrochemistry and Multifunctional Imaging: Scanning Electrochemical Cell Microscopy. *Analytical Chemistry*. **82** (22), 9141-9145 (2010).

- 42 Ebejer, N. et al. Scanning Electrochemical Cell Microscopy: A Versatile Technique for Nanoscale Electrochemistry and Functional Imaging. *Annual Review of Analytical Chemistry*. **6** (1), 329-351 (2013).
- 43 Alheshibri, M., Qian, J., Jehannin, M., Craig, V. S. A history of nanobubbles. *Langmuir*. **32** (43), 11086-11100 (2016).
- 44 Liu, G., Wu, Z., Craig, V. S. Cleaning of protein-coated surfaces using nanobubbles: an investigation using a quartz crystal microbalance. *The Journal of Physical Chemistry C*. **112** (43), 16748-16753 (2008).
- 45 Ghadimkhani, A., Zhang, W., Marhaba, T. Ceramic membrane defouling (cleaning) by air Nano Bubbles. *Chemosphere*. **146** 379-384 (2016).
- 46 Uchida, T. et al. Transmission electron microscopic observations of nanobubbles and their capture of impurities in wastewater. *Nanoscale Research Letters*. **6** (1), 1 (2011).
- 47 Ushikubo, F. Y. et al. Evidence of the existence and the stability of nano-bubbles in water. *Colloids and Surfaces A: Physicochemical and Engineering Aspects*. **361** (1-3), 31-37 (2010).
- 48 Bowley, W. W., Hammond, G. L. Controlling factors for oxygen transfer through bubbles. *Industrial, Engineering Chemistry Process Design and Development*. **17** (1), 2-8 (1978).
- 49 Li, P., Takahashi, M., Chiba, K. Enhanced free-radical generation by shrinking microbubbles using a copper catalyst. *Chemosphere*. **77** (8), 1157-1160 (2009).
- 50 Takahashi, M. et al. Effect of shrinking microbubble on gas hydrate formation. *The Journal of Physical Chemistry B*. **107** (10), 2171-2173 (2003).
- 51 Takahashi, M., Chiba, K., Li, P. Free-radical generation from collapsing microbubbles in the absence of a dynamic stimulus. *The Journal of Physical Chemistry B*. **111** (6), 1343-1347 (2007).
- 52 Ahmed, A. K. A. et al. Influences of air, oxygen, nitrogen, and carbon dioxide nanobubbles on seed germination and plant growth. *Journal of Agricultural and Food Chemistry*. **66** (20), 5117-5124 (2018).
- 53 Zhang, D.-F. et al. Delicate control of crystallographic facet-oriented Cu₂O nanocrystals and the correlated adsorption ability. *Journal of Materials Chemistry*. **19** (29), 5220-5225 (2009).
- 54 Khaled Abdella Ahmed, A. et al. Colloidal Properties of Air, Oxygen, and Nitrogen Nanobubbles in Water: Effects of Ionic Strength, Natural Organic Matters, and Surfactants. *Environmental Engineering Science*. (2017).
- 55 Huang, Z. et al. PeakForce scanning electrochemical microscopy with nanoelectrode probes. *Microscopy Today*. **24** (6), 18-25 (2016).
- 56 Lou, S.-T. et al. Nanobubbles on solid surface imaged by atomic force microscopy. *Journal of Vacuum Science, Technology B: Microelectronics and Nanometer Structures Processing, Measurement, and Phenomena*. **18** (5), 2573-2575 (2000).
- 57 Borkent, B. M., Dammer, S. M., Schönherr, H., Vancso, G. J., Lohse, D. Superstability of surface nanobubbles. *Physical Review Letters*. **98** (20), 204502 (2007).
- 58 Agarwal, A., Ng, W. J., Liu, Y. Principle and applications of microbubble and nanobubble technology for water treatment. *Chemosphere*. **84** (9), 1175-1180 (2011).
- 59 Tasaki, T., Wada, T., Baba, Y., Kukizaki, M. Degradation of surfactants by an integrated nanobubbles/VUV irradiation technique. *Industrial & Engineering Chemistry Research*. **48** (9), 4237-4244 (2009).
- 60 Fujita, D., Itoh, H., Ichimura, S., Kurosawa, T. Global standardization of scanning probe microscopy. *Nanotechnology*. **18** (8), 084002 (2007).

659 61 Häßler-Grohne, W., Hüser, D., Johnsen, K.-P., Frase, C. G., Bosse, H. Current limitations of SEM
660 and AFM metrology for the characterization of 3D nanostructures. *Measurement Science and*
661 *Technology*. **22** (9), 094003 (2011).

662 62 Sakai, K. in *Measurement Techniques and Practices of Colloid and Interface Phenomena*. 51-
663 57 (Springer, 2019).

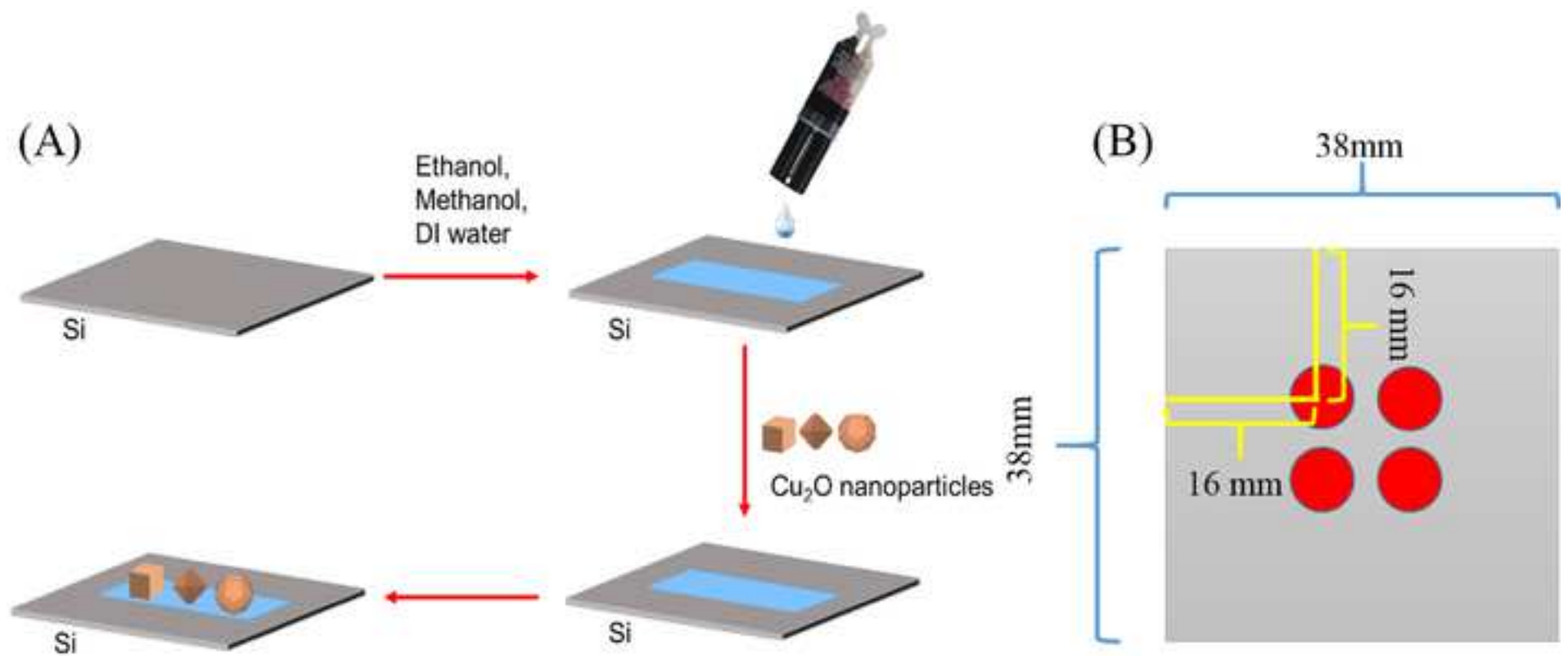
664 63 Gan, T., Wu, B., Zhou, X., Zhang, G. Ultrahigh resolution, serial fabrication of three
665 dimensionally-patterned protein nanostructures by liquid-mediated non-contact scanning probe
666 lithography. *RSC Advances*. **6** (55), 50331-50335 (2016).

667 64 Arteaga, J. F. et al. Comparison of the simple cyclic voltammetry (CV) and DPPH assays for the
668 determination of antioxidant capacity of active principles. *Molecules*. **17** (5), 5126-5138 (2012).

669 65 Moreno-Herrero, F., Colchero, J., Gomez-Herrero, J., Baro, A. Atomic force microscopy contact,
670 tapping, and jumping modes for imaging biological samples in liquids. *Physical Review E*. **69** (3),
671 031915 (2004).

672 66 Doktycz, M. et al. AFM imaging of bacteria in liquid media immobilized on gelatin coated mica
673 surfaces. *Ultramicroscopy*. **97** (1-4), 209-216 (2003).

674



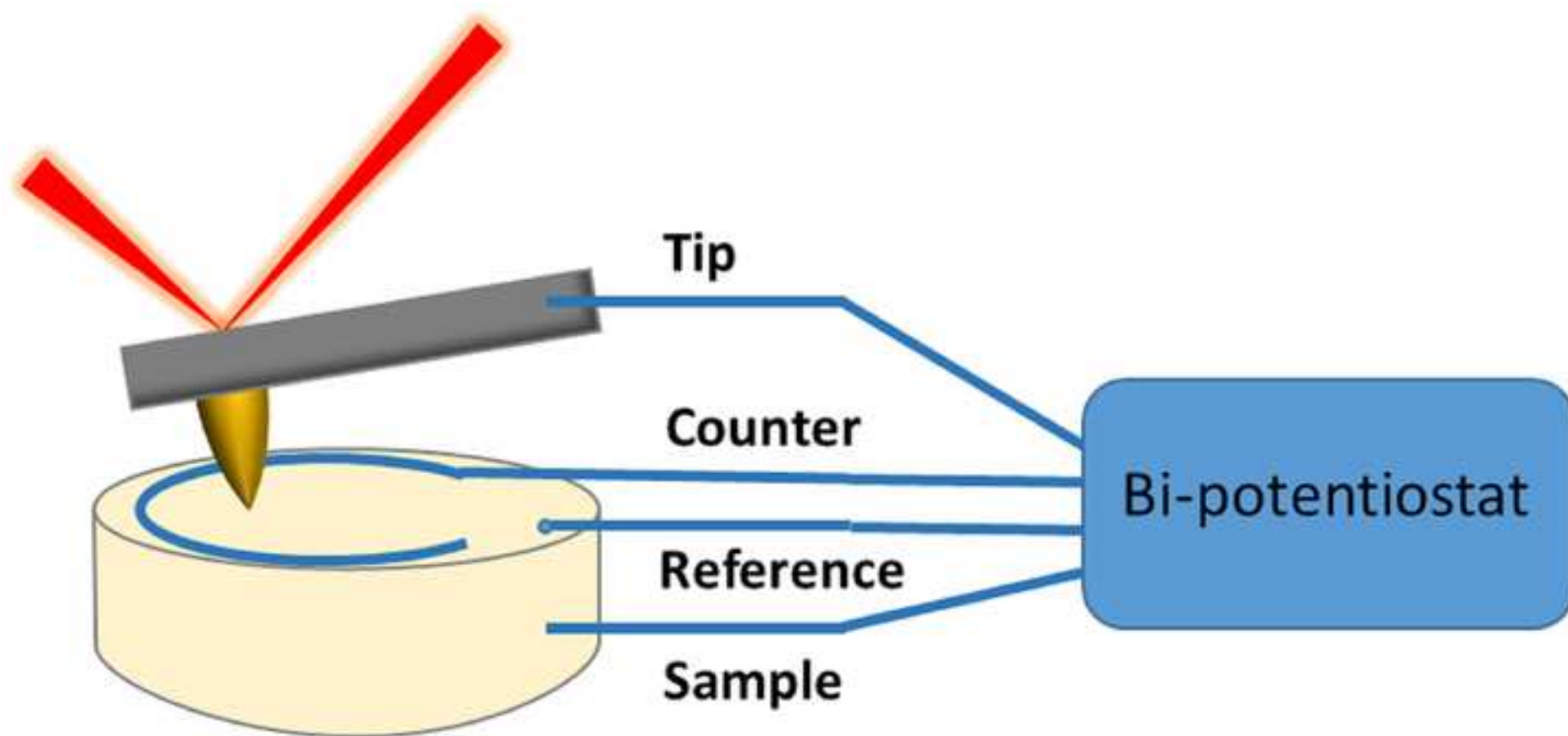


Figure 3

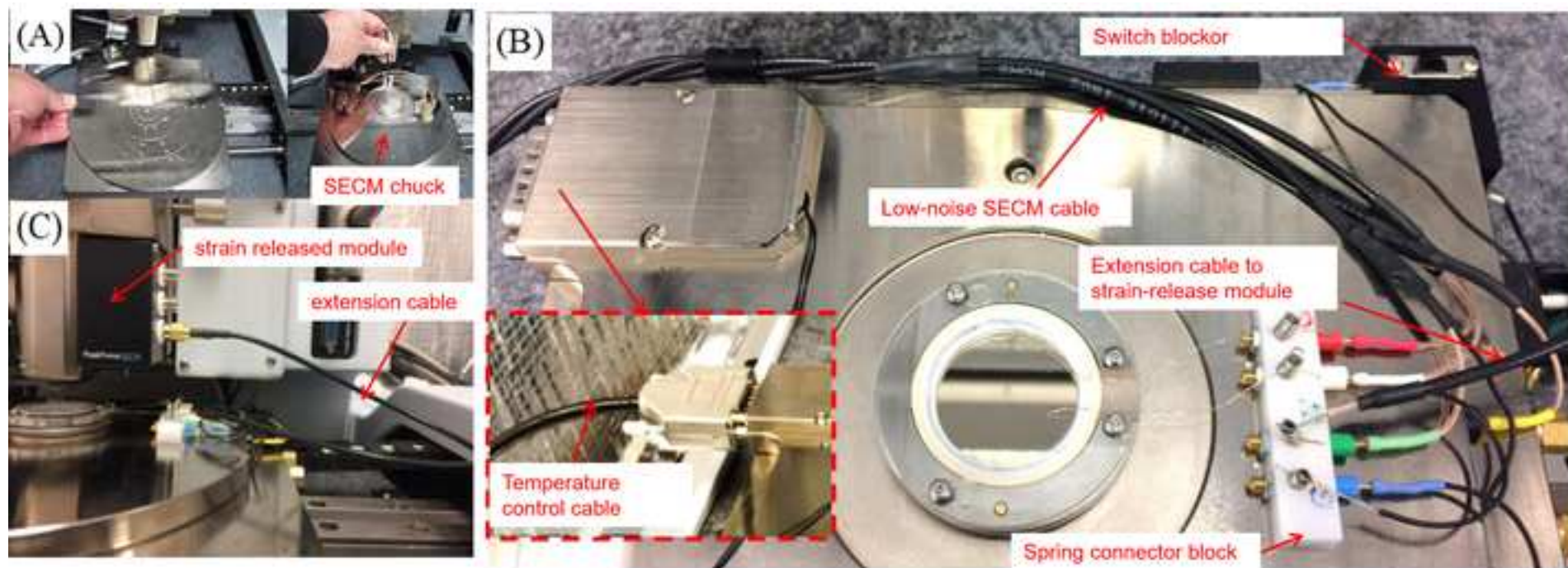


Figure 4

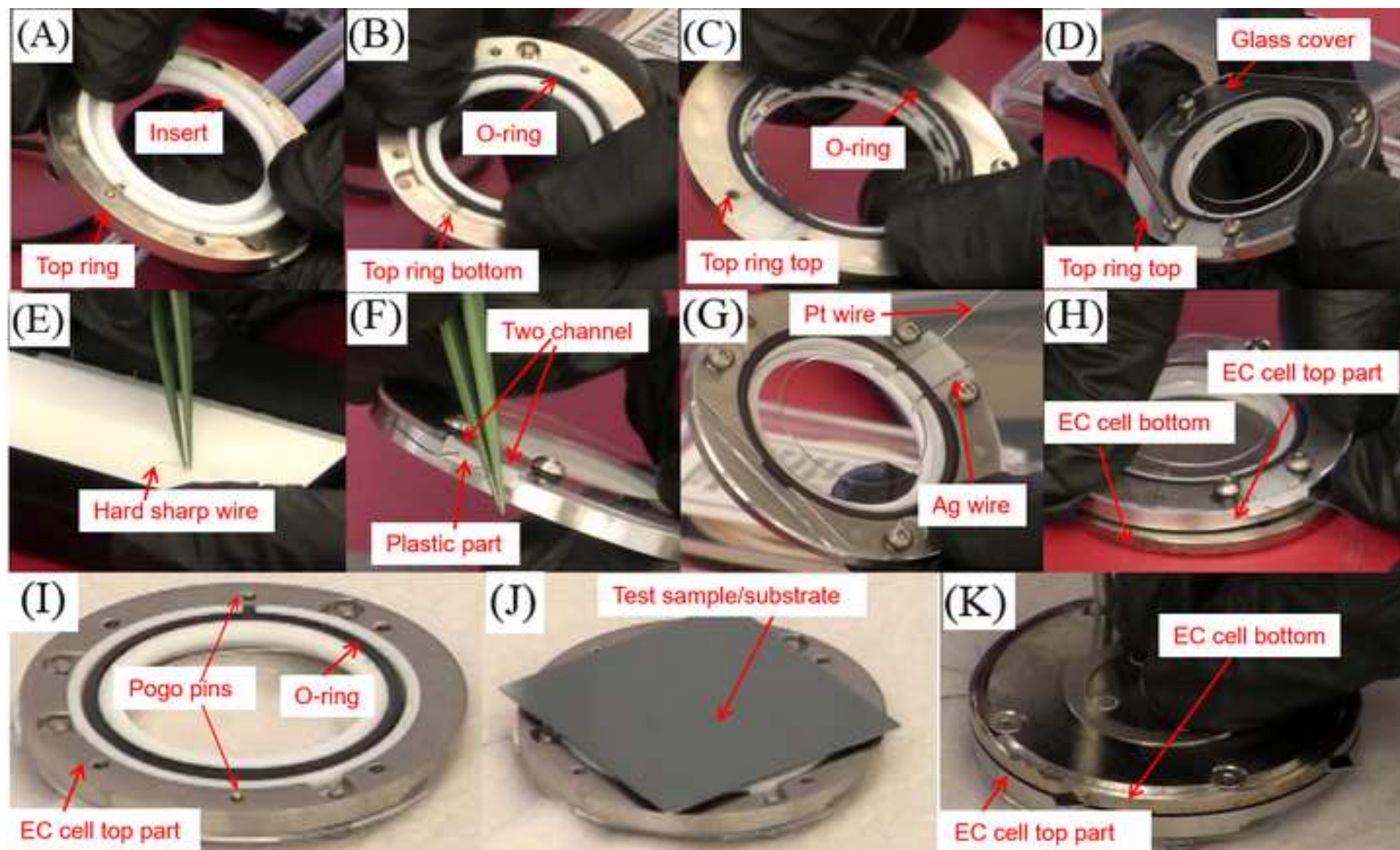
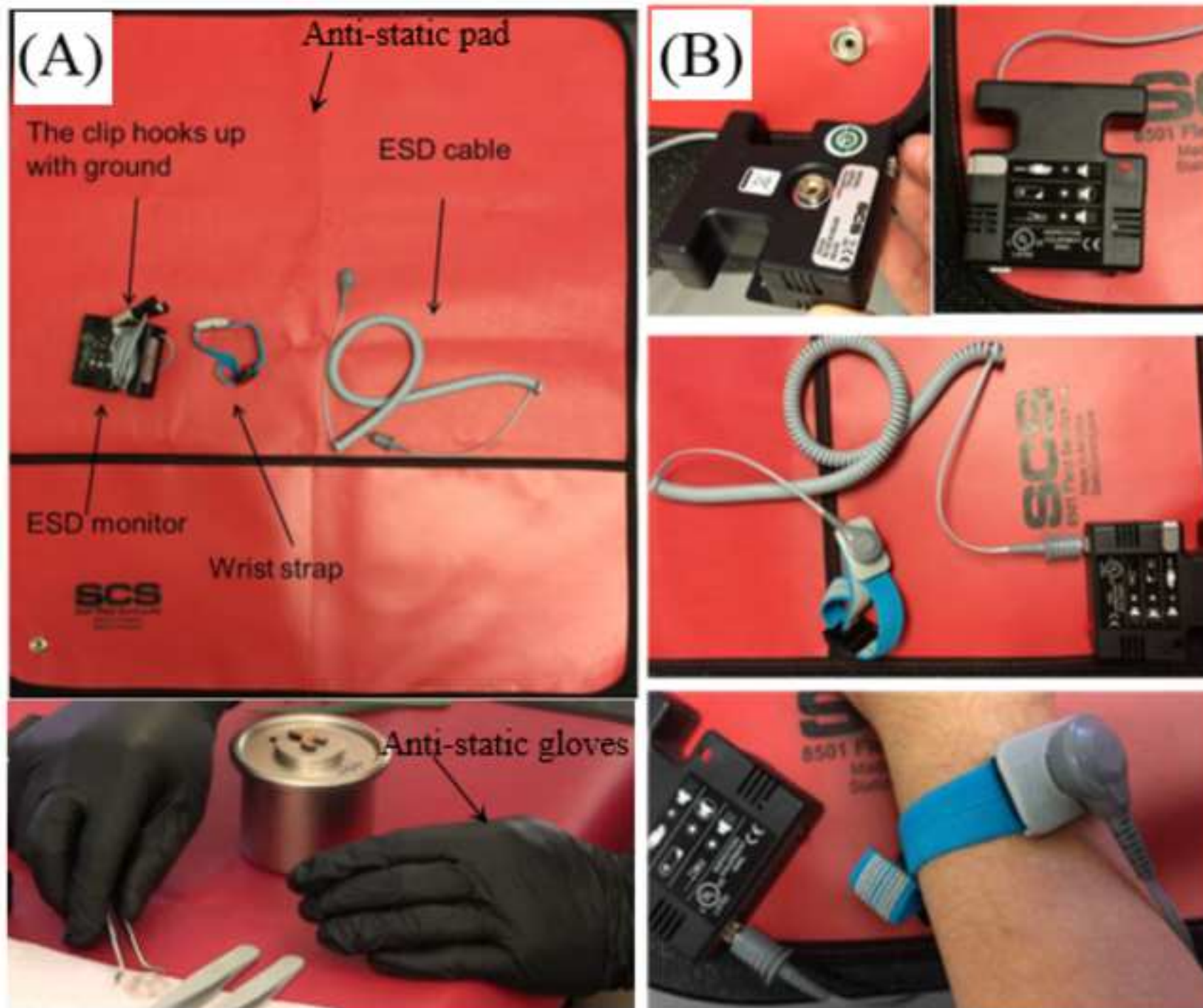
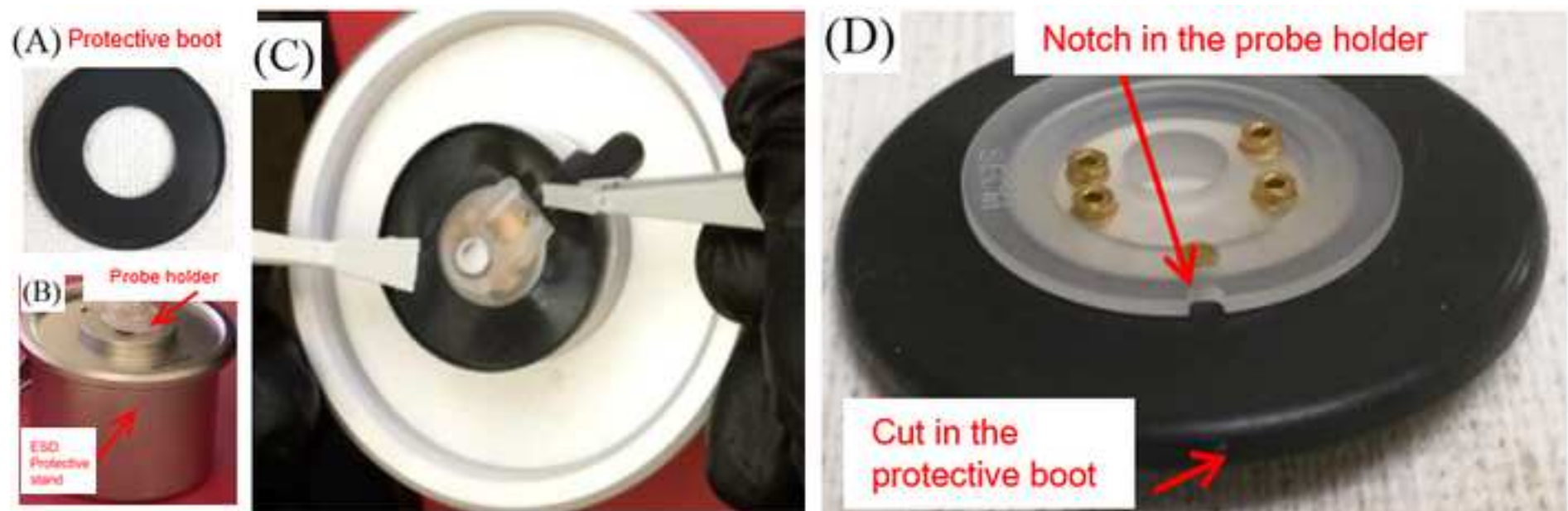
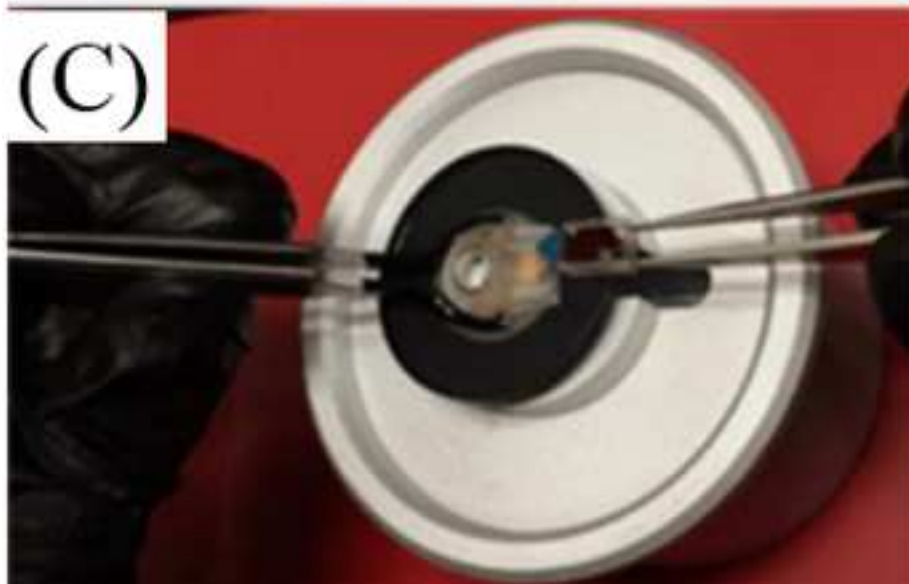
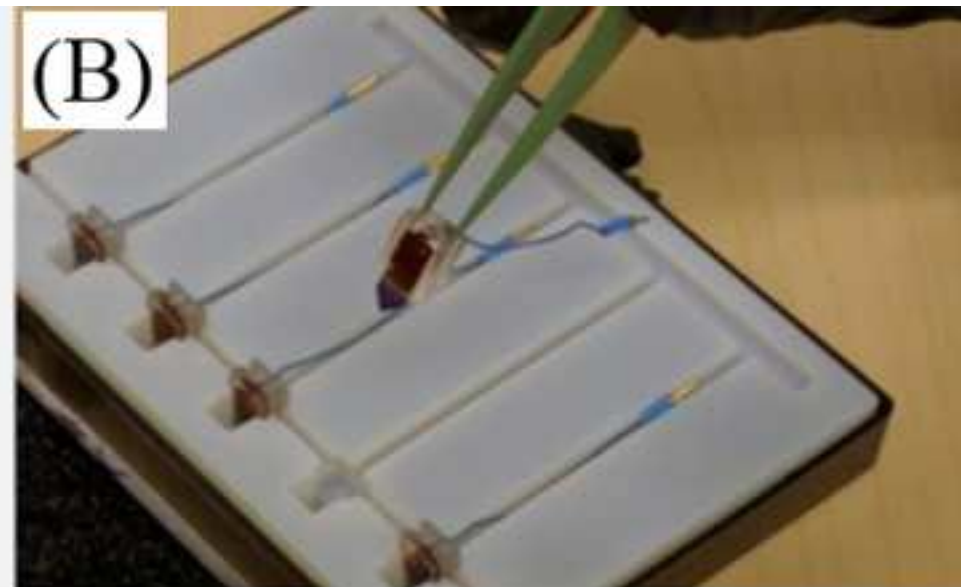
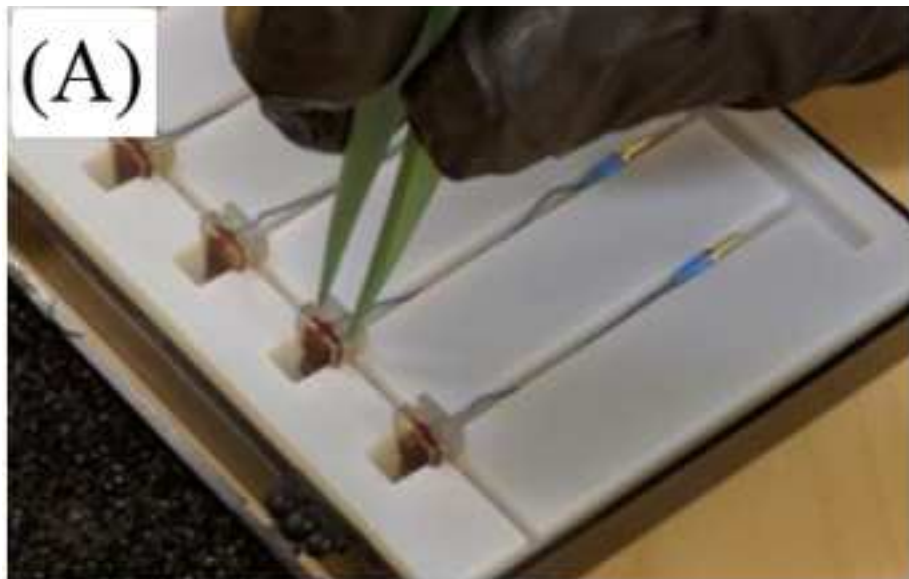


Figure 5







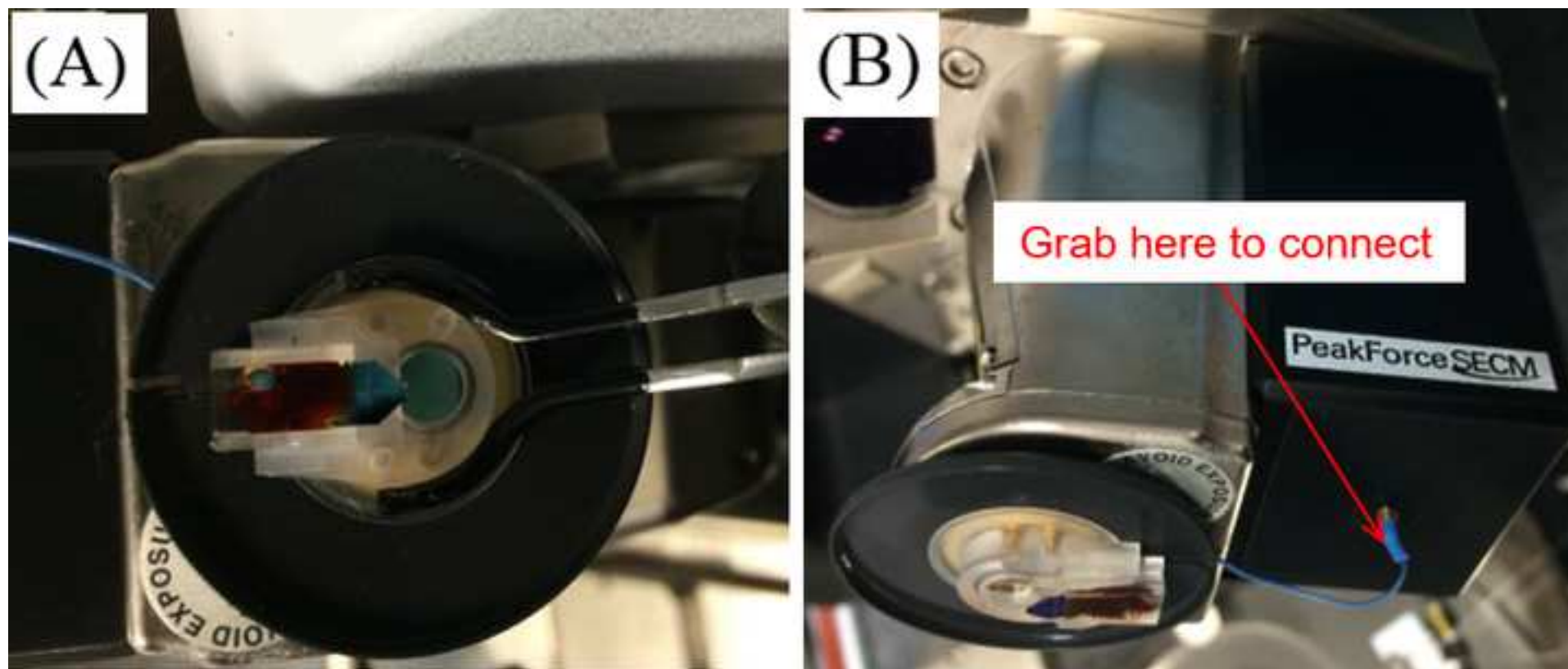


Figure 9

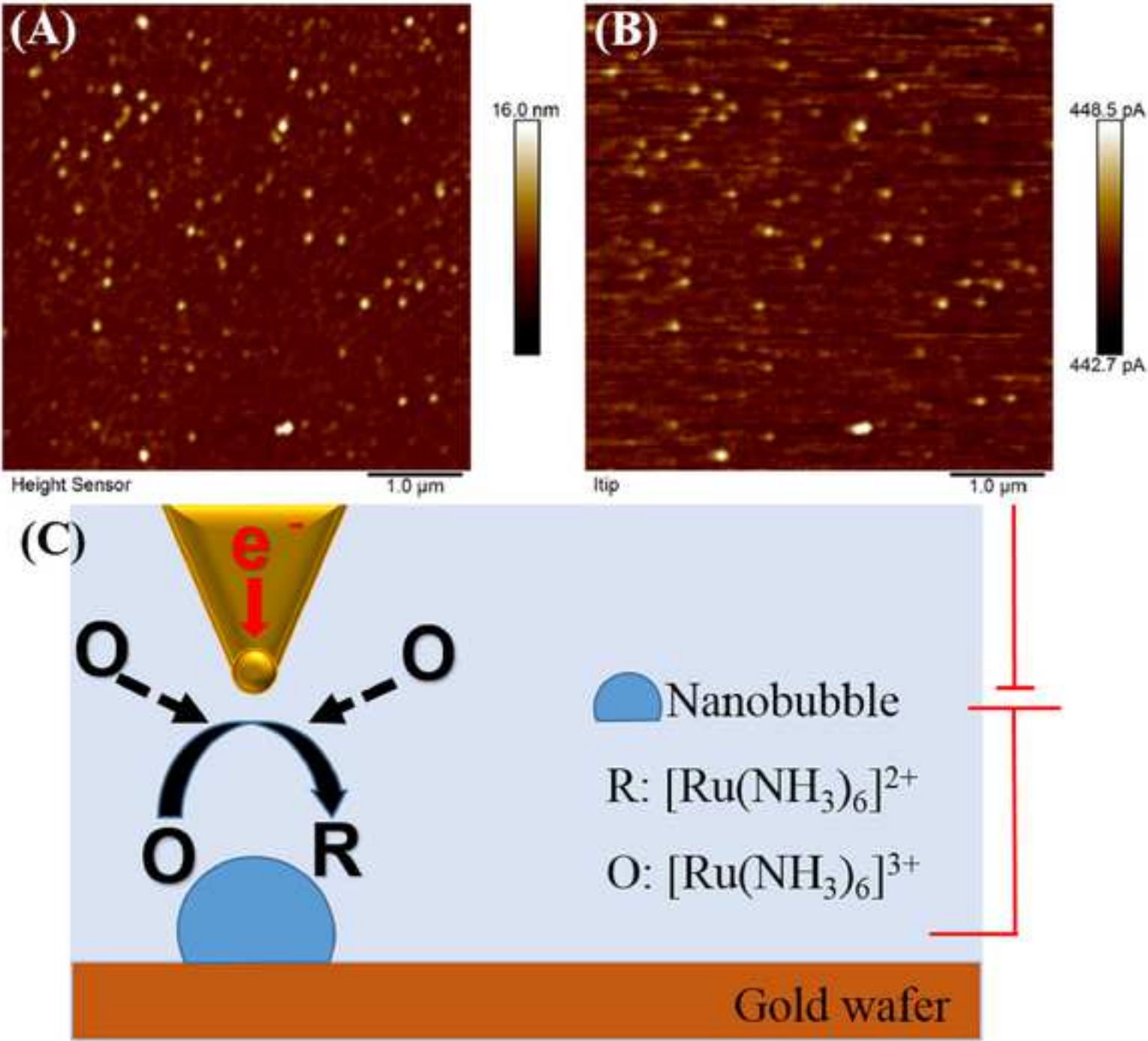
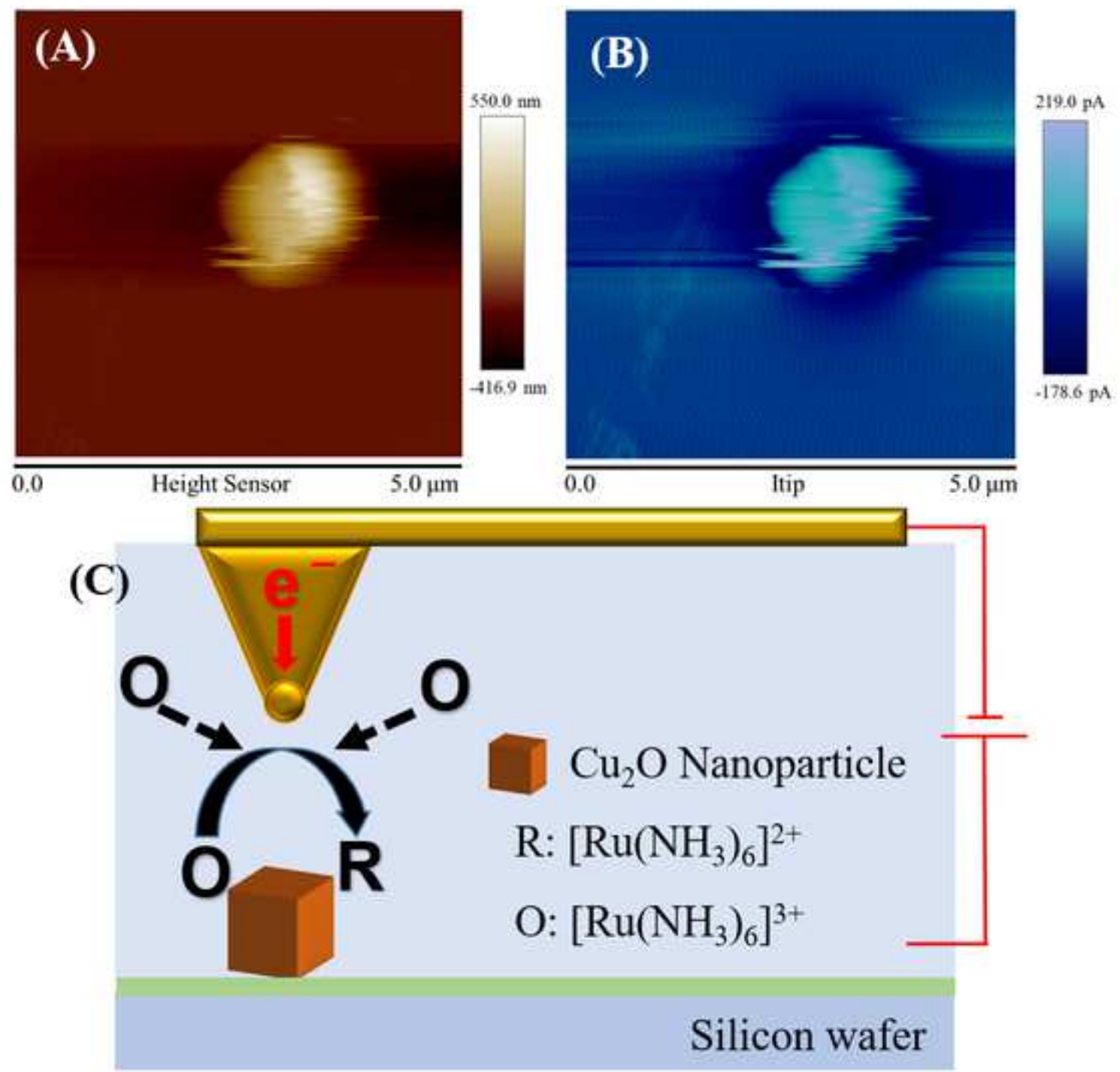
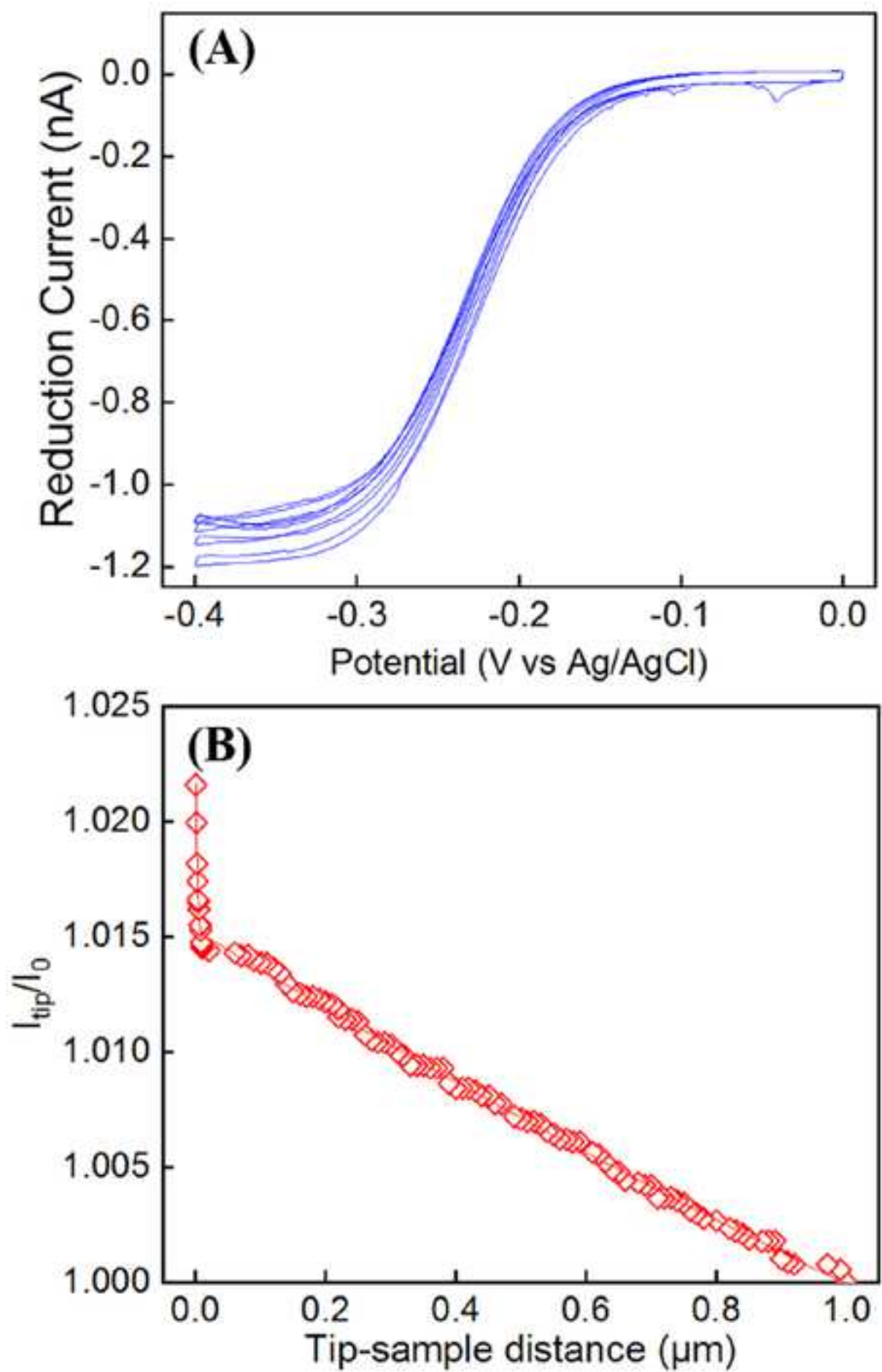


Figure 10





Name of Material/ Equipment	Company	Catalog Number	Comments/Description
Equipment			
Atomic force microscopy	Bruker, CA	Dimenison Icon	
Bipotentiostat	CH Instruments, Inc.	CHI 700E	
Materials			
Silicon wafer	TED PELLA, Inc.	16013	
Fresh gold plates	Bruker, CA	model 119-017-307	
PF-SECM-AFM probes	Bruker, CA	990-050138	
PF-SECM strain-release module	Bruker, CA	840-012-724	
PF-SECM Probe Holder	Bruker, CA	900-050121	
PF-SECM Chuck	Bruker, CA	PF-SECM Chuck	
PF-SECM O-ring	Bruker, CA	598-000-106	
PF-SECM cover glass, SECM Cell	Bruker, CA	900-050137	
EC Cell Assy	Bruker, CA	932-017-300	
ESD Field Service	Bruker, CA	490-000-066	
PF-SECM Boot	Bruker, CA	900-050136	
Spring connector block	Bruker, CA	900-050524	
PFSECM Tweezers	Bruker, CA		
Cable, SECM Tip module	Bruker, CA	468-050171	
Ag wire	Bruker, CA	249-000-056	
Pt wire	Bruker, CA	248-000-004	
Hard sharp wire	Bruker, CA	TT-ECM10	
Tubular ceramic membrane	Refracton	WFA0.1	
Chemicals			
Copper(II) chloride dihydrate	ACROS Organics	AC315281000	
Sodium Hydroxide	Fisher Chemical	S318-100	
Ascorbic Acid	Fisher Chemical	A61-25	
Epoxy	Loctite	Instant Mix	
Potassium Chloride	Fisher Chemical	P217-500	
Hexaammineruthenium(III) chloride	ACROS Organics	AC363342500	

**NEWARK COLLEGE OF ENGINEERING**

New Jersey Institute of Technology
University Heights
Newark, NJ 07102
(973) 596-2444/2447
(973) 596-5790 fax

Department of Civil and
Environmental Engineering

March 15, 2020

Manuscript ID: JoVE61111

Title: Probing Surface Electrochemical Activity of Nanomaterials using Hybrid Atomic Force Microscope-Scanning Electrochemical Microscope (AFM-SECM)

Dear Editor(s),

Thank you very much for giving us the opportunity to revise and resubmit our manuscript. The comments and suggestions made on our manuscript by the reviewers were encouraging and helpful. We have addressed all these major points and other issues carefully and revised the manuscript accordingly. We provide detailed responses to the editors' comments in the following pages.

Please note that the editors' comments are presented in *italics*, and our responses are in Roman and blue font. All changes made to the manuscript accordingly are marked in red font in the manuscript. Please let me know if you have any further questions. Thank you for your consideration.

Best regards,

A handwritten signature in black ink, appearing to be 'Wen Zhang'.

Wen Zhang, Ph.D., P.E., BCEE
Associate Professor
Department of Civil and Environmental Engineering
Department of Chemical and Material Engineering
New Jersey Institute of Technology
323 Martin Luther King Blvd. Newark, NJ 07102
Office Phone: (973) 596-5520
Email: wen.zhang@njit.edu

Response to the Editor comments

We appreciate the editor for the constructive comments.

1. *Please highlight up to 2.75 pages of protocol text for inclusion in the video. This is a hard production limit to ensure that videography can occur in a single day. Please ensure that sufficient details are highlighted to tell a full and cohesive story about the protocol.*

Response:

The protocol has been highlighted for critical steps and the highlighted protocol is less than 2.75 pages.

2. *Please provide a title for each figure.*

Response:

The titles of each figure and table are provided below. The titles are also provided in the manuscript (Line 419 to Line 446).

Fig. 1 Deposition of Cu₂O nanoparticles on a silicon wafer.

Fig. 2 Schematic of AFM-SECM system

Fig. 3 Installation procedure for SECM chuck and other accessories.

Fig. 4 Assemblage procedure of the EC sample cell.

Fig. 5 (A) Parts of ESD protective parts; (B) Connections of ESD monitor, wrist strap and ground wire.

Fig. 6 Attachment procedure for the protective boot onto the probe holder

Fig. 7 Loading the SECM probe to the probe holder

Fig. 8 (A) Attach the probe-holder-boot assembly to the scanner; (B) Connection of probe to the strain released module.

Fig. 9 Simultaneously acquired topography (A) and tip current (B) images of oxygen NBs in electrolyte containing 10 mM [Ru(NH₃)₆]³⁺ and 0.1 M KCl. The tip (end tip radius is 25nm) was biased at -0.4V. (C) Schematic illustration of AFM-SECM measurement of NBs

Fig. 10 Simultaneously acquired topography (A) and tip current (B) images of Cu₂O nanoparticles in electrolyte containing 10 mM [Ru(NH₃)₆]³⁺ and 0.1 M KCl. The tip (end tip radius is 25nm) was biased at -0.4V (C) Schematic illustration of AFM-SECM measurement of NPs.

Fig. 11 (A) Five CV scan in 10 mM [Ru(NH₃)₆]³⁺ and 0.1 M KCl. (B) Approach curves of nanoelectrode probe on Cu₂O nanoparticle surface.

Table 1 Examples of redox mediators used in literature.

Fig. S1 Photo showing connection between the bipotentiostat and the AFM controller.

Fig. S2 Load the PeakForce SECM workspace in the software

Fig. S3 Navigation panel for SECM workspace.

Fig. S4 Run Open Circuit Potential – Time

Fig. S5 Run Cyclic Voltammetry

Fig. S6 Parameter setting for cyclic voltammetry measurement

Fig. S7 Parameters for a Chronoamperometry measurement

Fig. S8 Start current reading in AFM-SECM software

Fig. S9 Parameters for Amperometric i-t technique

3. *Please revise the Table of Materials to ensure that all materials and equipment are included.*

Response:

The Table of Materials contained all materials and equipment.

4. *There are scattered typos throughout. The manuscript would benefit from an additional read-over.*

Response:

The manuscript has been checked and typos were corrected.

5. *Please upload Table 1 as an xls/xlsx file.*

Response:

The Table 1 is uploaded as an excel file along with other revised materials.

.

Figure S1


[Click here to access/download;Supplemental File \(Figures, Permissions, etc.\);Fig. S1.png](#)



Select Experiment: Dimension Icon

1


Select From:

☐  Use previous experiment


SECM - PeakForce QNM - 04/24/18 | 20:28

Or


Choose an Experiment Category:

 Scan Asyst


ScanAsyst

 Tapping Mode


Tapping Mode

 Contact Mode


Contact Mode

 Electrical & Magnetic


Electrical & Magnetic

 Mechanical Properties

Mechanical Properties


 Electroche...

Electroche...

 Other SPM

Other SPM

Microscope: Dimension Icon



[>> Change Scanner](#)

[>> Change Microscope Setup](#)

2

Select Experiment Group:

EC

SECM

3

Select Experiment:


SECM - Contact Mode

SECM - PeakForce QNM

SECM - ScanAsyst

Cancel

☐ Ignore Probe Parameters

 Load Experiment

Experiment Description

AFM-SECM requires a nanoelectrode with tip dimensions in sub-micron or even sub 100 nm, which enable true nanoscale resolution. PeakForce SECM is based on Bruker developed batch-fabricated, high-quality, SECM probes referred to as a nanoelectrode having tip diameter of approximately 50 nm. With these probes, PeakForce SECM scanning is obtained, which simultaneously provides topographical, electrical, and quantitative mechanical maps on the nanometer-scale, along with electrochemical images of less than 100-nm resolution. In addition, it also provides unique capabilities for high-quality nanoelectrical imaging in liquid by use of the high-bandwidth electronics from PeakForce-enabled electrical modes in air. Sub-nanometer electrochemical reactivity is realized utilizing the AFM's precise tip positioning and an interleave mode scan. In the main scan,

Focus Sample

1.1 Select Focus Method

Sample (default)

Tip Reflection

1.2 Autocompensate for fluid (only if focus is done in fluid)

1.3 Adjust focus by moving scan head up or down

Scan Head

Speed

12.0%

Be careful, adjusting focus position too fast may cause tip to contact surface

Navigate to Scan Centerpoint

2.1 Navigate to a region of interest

XY Control

Speed

14.0%

2.2 Teach EC Blind Engage Position

Update Blind Engage Position

Blind Engage Position X: 81495.8 μ m

Blind Engage Position Y: 157727 μ m

Blind Engage Position Z: -11524.5 μ m

If sample is changed or moved the EC Blind Engage Position must be retaught

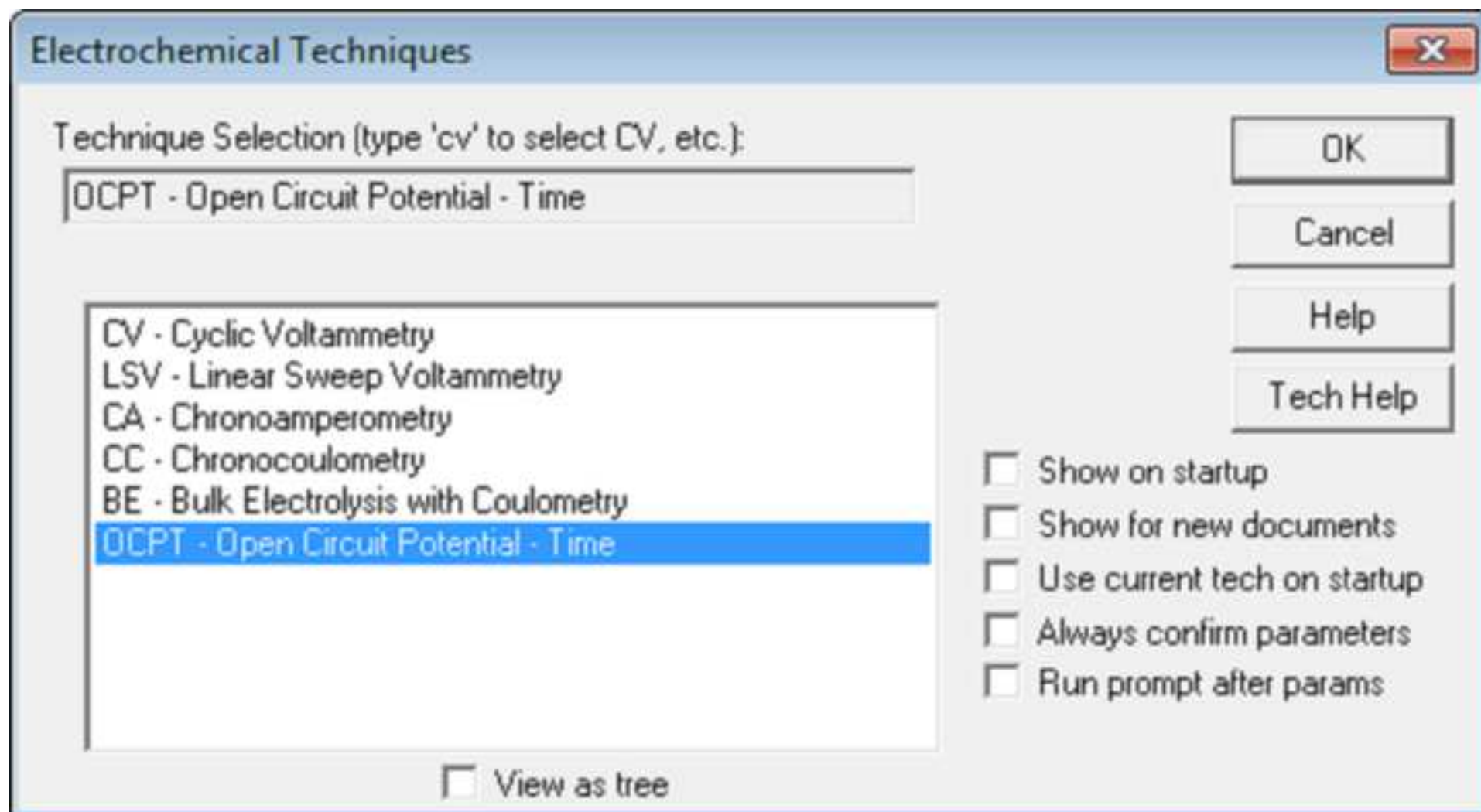
EC Fluid Mode Navigation

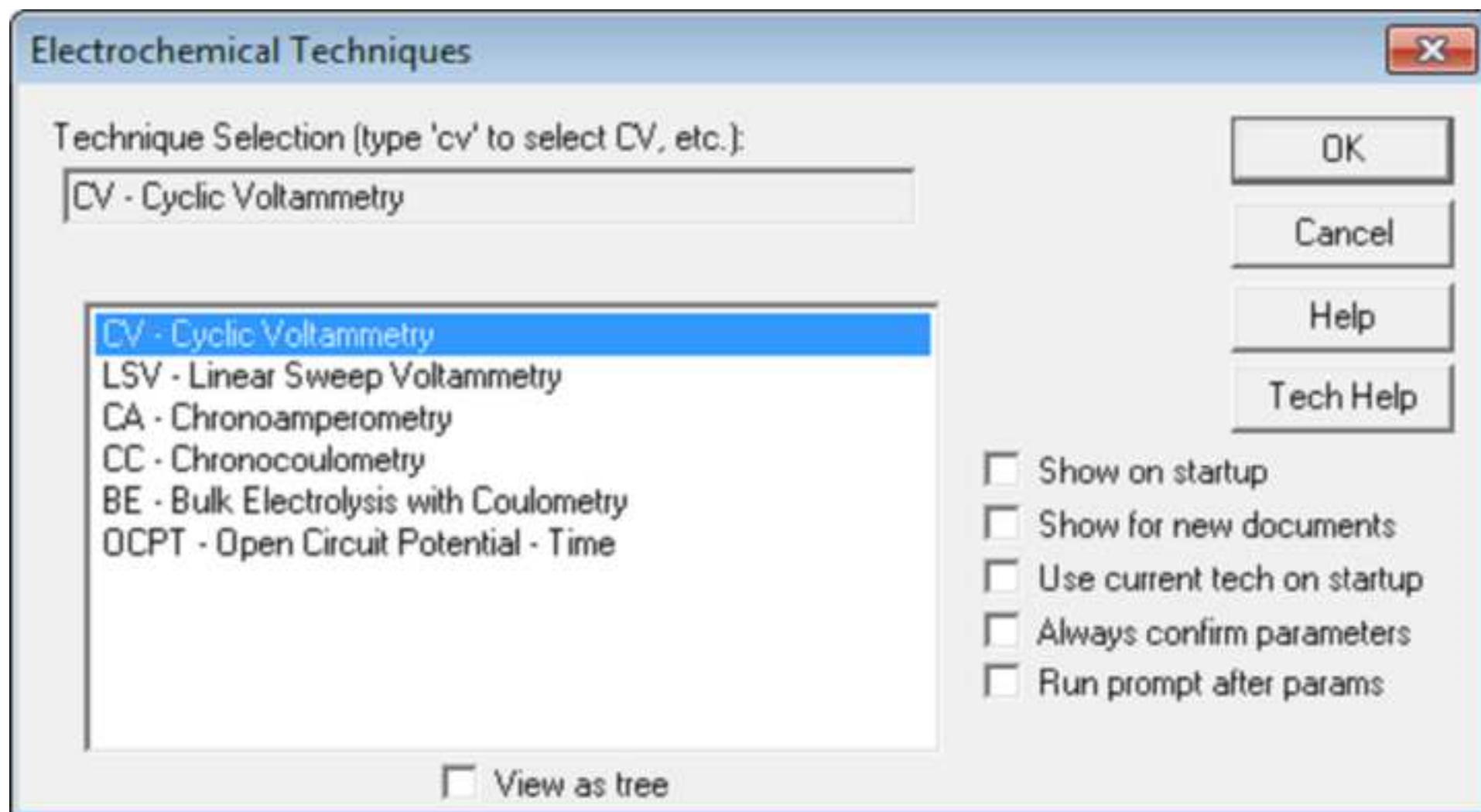
3.1 Move to Add Fluid Position

Move to Add Fluid Position

3.2 Move to Blind Engage Position

Move to Blind Engage Position





Cyclic Voltammetry Parameters ✕

Init E (V)	<input type="text" value="0"/>	<input type="button" value="OK"/> <input type="button" value="Cancel"/> <input type="button" value="Help"/>
High E (V)	<input type="text" value="0"/>	
Low E (V)	<input type="text" value="-0.4"/>	
Final E (V)	<input type="text" value="-0.4"/>	
Initial Scan Polarity.....	<input type="text" value="Negative"/> ▼	
Scan Rate (V/s)	<input type="text" value="0.05"/>	
Sweep Segments	<input type="text" value="10"/>	
Sample Interval (V)	<input type="text" value="0.001"/>	
Quiet Time (sec)	<input type="text" value="2"/>	
Sensitivity (A/V)	<input type="text" value="1.e-009"/> ▼	

Electrode 2

Potential (V)	<input type="text" value="0"/>	<input checked="" type="radio"/> Off
Differential E (V)	<input type="text" value="0"/>	<input type="radio"/> Constant E
Sensitivity (A/V)	<input type="text" value="1.e-006"/> ▼	<input type="radio"/> Scan
		<input type="radio"/> Diff Scan

☐ Swap Electrode 1 and 2 if Scan Rate is ≤ 25 V/s

☐ Auto Sens if Scan Rate ≤ 0.01 V/s

☐ Enable Final E

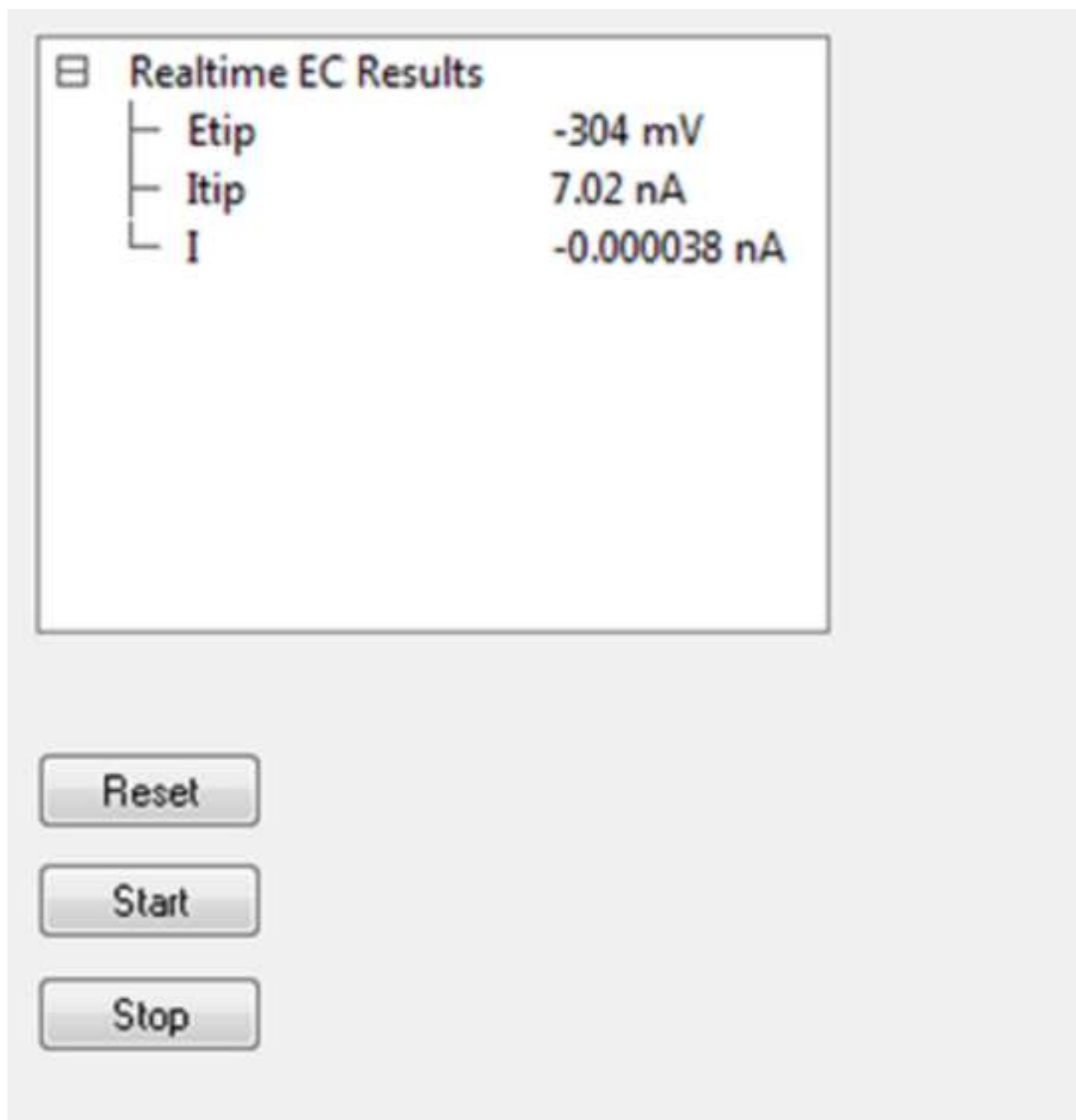
☐ Auxiliary Signal Recording

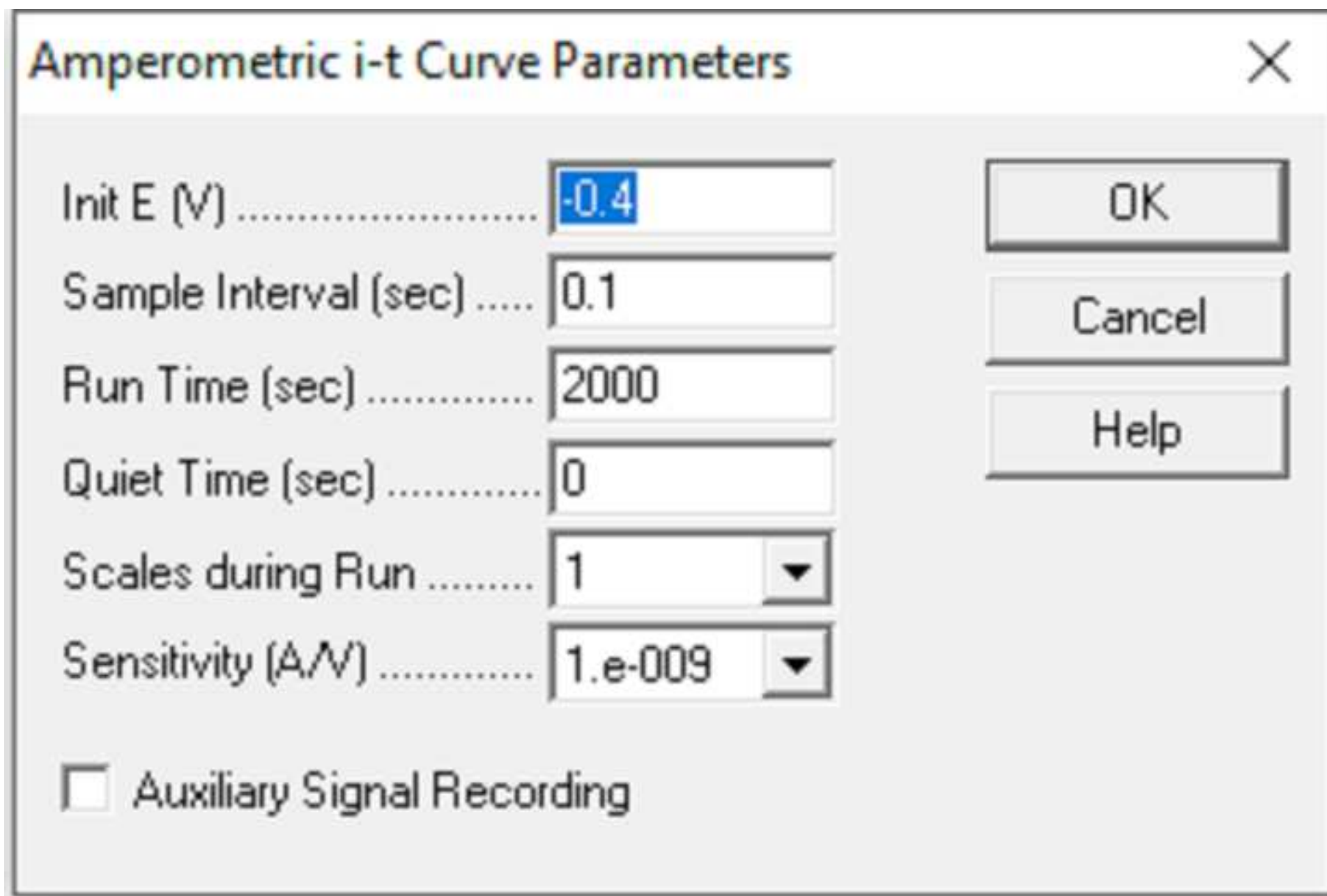
Chronoamperometry Parameters

Init E (V)	-0.4
High E (V)	-0.4
Low E (V)	-0.402
Initial Step Polarity.....	Negative ▼
Number of Steps	2
Pulse Width (sec)	1000
Sample Interval (sec)	0.001
Quiet Time (sec)	2
Sensitivity (A/V)	1.e-009 ▼

☐ Auxiliary Signal Recording When Sample Interval ≥ 0.005 s

OK
Cancel
Help





A dialog box titled "Amperometric i-t Curve Parameters" with a close button (X) in the top right corner. The dialog contains several input fields and a checkbox. The input fields are arranged in a list on the left, each followed by a text box for the value. The values are: Init E (V) = -0.4, Sample Interval (sec) = 0.1, Run Time (sec) = 2000, Quiet Time (sec) = 0, Scales during Run = 1, and Sensitivity (A/V) = 1.e-009. The last two fields have dropdown arrows. On the right side of the dialog, there are three buttons: OK, Cancel, and Help. At the bottom left, there is a checkbox labeled "Auxiliary Signal Recording" which is currently unchecked.

Parameter	Value
Init E (V)	-0.4
Sample Interval (sec)	0.1
Run Time (sec)	2000
Quiet Time (sec)	0
Scales during Run	1
Sensitivity (A/V)	1.e-009

☐ Auxiliary Signal Recording

OK
Cancel
Help

Reaction	E ₀ / V	Concentration
\rightleftharpoons $2\text{H}^{+} + 2\text{e}^{-} \rightarrow \text{H}_2$	0	
\rightleftharpoons $[\text{Ru}(\text{NH}_3)_6]^{3+} + \text{e}^{-} \rightarrow [\text{Ru}(\text{NH}_3)_6]^{2+}$	0.10 (NHE)	10 mM
\rightleftharpoons $2\text{NO}_2^{-} + 3\text{H}_2\text{O} + 4\text{e}^{-} \rightarrow \text{N}_2\text{O} + 6\text{OH}^{-}$	0.15(NHE)	0.1 M
\rightleftharpoons $[\text{Fe}(\text{CN})_6]^{3-} + \text{e}^{-} \rightarrow [\text{Fe}(\text{CN})_6]^{4-}$	0.358(NHE)	2~5 mM
\rightleftharpoons $\text{ClO}_4^{-} + \text{H}_2\text{O} + 2\text{e}^{-} \rightarrow \text{ClO}_3^{-} + 2\text{OH}^{-}$	0.36(NHE)	0.1~1 M
\rightleftharpoons $[\text{IrCl}_6]^{3-} + 3\text{e}^{-} \rightarrow \text{Ir} + 6\text{Cl}^{-}$	0.77(NHE)	10 mM
\rightleftharpoons $\text{SO}_4^{2-} + \text{H}_2\text{O} + 2\text{e}^{-} \rightarrow \text{SO}_3^{2-} + 2\text{OH}^{-}$	-0.93 (NHE)	10 mM
\rightleftharpoons $\text{AgCl} + \text{e}^{-} \rightarrow \text{Ag} + \text{Cl}^{-}$	0.22233(NHE)	

References:

1. Jiang, J. et al. Nanoelectrical and Nanoelectrochemical Imaging of Pt/p-Si and Pt/p+-Si Electrodes. ChemSusChen

2.Izquierdo, J., Eifert, A., Kranz, C. & Souto, R. M. In situ monitoring of pit nucleation and growth at an iron passive

3. Jones, C. E., Unwin, P. R. & Macpherson, J. V. In situ observation of the surface processes involved in dissolution
146 (2002)
4. Anne, A., Cambril, E., Chovin, A., Demaille, C. & Goyer, C. Electrochemical atomic force microscopy using a tip-at
5. Macpherson, J. V., Jones, C. E., Barker, A. L. & Unwin, P. R. Electrochemical imaging of diffusion through single n:
6. Izquierdo, J., Eifert, A., Kranz, C. & Souto, R. M. In situ investigation of copper corrosion in acidic chloride solutio

Applied Potential	Ref
-0.4 V (Ag/AgCl)	1
+0.95V (Ag/AgCl)	2
+0.0 ~ 0.5V(Ag/AgCl)	3
+0.30 V(SCE)	4
+1.0 V(Ag/AgCl)	5
-0.45 V(Ag/AgCl)	6

n. 10 (22), 4657-4663, (2017).

oxide layer by using combined atomic force and scanning electrochemical microscopy. ChemEl

from the cleavage surface of calcite in aqueous solution using combined scanning electrochemical microscopy and a redox mediator for topographic and functional imaging of nanosystems. ACS nano. 3 (10), 3981-3988, (2009).

nanoscale pores. Analytical chemistry. 74 (8), 1841-1848, (2002).

on using atomic force—scanning electrochemical microscopy. Electrochimica Acta. 247 588-599, (2007).

anical-Atomic Force microscopy (SECIM-AFM). ChemPhysChem. 4 (2), 159-
), 2927-2940, (2009).

(2017).